Bioorganic Chemistry 101 (2020) 103960

Contents lists available at ScienceDirect

Bioorganic Chemistry

journal homepage: www.elsevier.com/locate/bioorg

Design, synthesis and evaluation of benzothiazole derivatives as multifunctional agents

Ernestine Nicaise Djuidje[a], Sabrina Sciabica[b], Raissa Buzzi[a], Valeria Dissette[a], Jan Balzarini[c], Sandra Liekens[c], Elena Serra[a,e], Elisa Andreotti[d], Stefano Manfredini[a], Silvia Vertuani[a,*], Anna Baldisserotto[a]

[a] Department of Life Sciences and Biotechnology, Master Course in Cosmetic Science and Technologies, University of Ferrara, via L. Borsari 46, 44121 Ferrara, Italy
[b] Department of Chemical and Pharmaceutical Sciences, University of Ferrara, via F. di Mortara 17-19, 44121 Ferrara, Italy
[c] Department of Microbiology and Immunology, KU Leuven, University of Leuven, Rega Institute for Medical Research, Laboratory of Virology and Chemotherapy, Leuven B-3000, Belgium
[d] Department of Life Sciences, University of Modena and Reggio Emilia, Via Giuseppe Campi 287, 41125 Modena, Italy
[e] Aptuit, An Evotec Company, Via A. Fleming 4, 37135 Verona, Italy

ARTICLE INFO

Keywords:
Benzothiazoles
Antioxidant
UV-filter
Antifungal
Antiproliferative
hERG channels

ABSTRACT

Oxidative stress is the product or aetiology of various multifactorial diseases; on the other hand, the development of multifunctional compounds is a recognized strategy for the control of complex diseases. To this end, a series of benzothiazole derivatives was synthesized and evaluated for their multifunctional effectiveness as antioxidant, sunscreen (filter), antifungal and antiproliferative agents. Compounds were easily synthesized via condensation reaction between 2-aminothiophenols and different benzaldehydes. SAR study, particularly in position 2 and 6 of benzothiazoles, led to the identification of **4g** and **4k** as very interesting potential compounds for the design of multifunctional drugs. In particular, compound **4g** is the best blocker of hERG potassium channels expressed in HEK 293 cells exhibiting 60.32% inhibition with IC_{50} = 4.79 μM.

1. Introduction

Multifactorial diseases, such as cancer, are caused by a combination of genetic and/or environmental factors and have complex pathological mechanisms. However, it is not always easy to find drugs that can act on different sites. Several approaches, including cocktails of drugs, were developed for the extension of prevention and effective therapy, as well as reduction of the disease complications. Nevertheless, these methodologies were found to be inefficient due to their complex side effects and the unbalance between pharmacokinetic and pharmacodynamic relationships. Nowadays a new approach to the problem consists in the design and development of a single multifunctional chemical entity [1,2] (see Fig. 1).

Environmental factors that can cause multifactorial diseases include exposure to ultraviolet radiation (UVR) or other forms of radiation (e.g. X-rays, gamma rays), pollution and related chemical substance, viruses, bacterial and fungal infections, diet and lifestyle. UV radiation (UVB and UVA) can damage cellular components (DNA, RNA, proteins, lipids, trans-urocanic acid and aromatic amino acids) contributing to the development of various skin diseases, including photoaging (accelerated skin and eyes aging) and cancer [3–5]. Furthermore, absorption of UVB by DNA bases induces the formation of cyclobutane pyrimidine dimers (CPDs) and pyrimidine-pyrimidone (6–4) photoproducts (6–4PPs) [6,7], while absorption of UVA induces the formation of photo-excited states of chromophores, generating reactive species that damage DNA [8]. Thus, UVA is a potent inducer of a variety of physiological changes characteristic of photoaging including chronic inflammation, immunosuppression and cancer [9]. In general, UV damage are also associated to ROS (reactive oxygen species) production, they are highly unstable and reactive molecules and for this reason they are readily detoxified or neutralized by biological system (enzymatic and non-enzymatic antioxidant). When ROS increase, the antioxidant defences could not be enough to neutralize the free-radical production inducing the oxidative stress. ROS react with lipids, nucleic acids and proteins, altering their cellular functions and contributing to many diseases.

Mycotoxins are very toxic for human and animal cells. Low molecular weight mycotoxins are soluble in lipids and can penetrate into skin creating damage to the cells, resulting specifically aflatoxin, carcinogenic to mankind. In addition, chronic aflatoxicosis lead to cancer and immune suppression [10]. Cells treated with mycotoxins (i.e.

* Corresponding author.
E-mail address: vrs@unife.it (S. Vertuani).

https://doi.org/10.1016/j.bioorg.2020.103960
Received 18 October 2019; Received in revised form 28 April 2020; Accepted 20 May 2020
Available online 02 June 2020

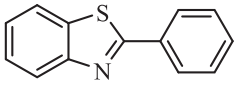

Fig. 1. Chemical structure of parent compound (**4a**).

ochratoxin A (OTA) and/or aflatoxin B1 (AFB1) produces high level of ROS and the use of antioxidant agents have shown to be effective in contrasting their cytotoxicity [11].

Therefore, it is important to develop products with the ability to prevent or inhibit the harmful effects of environmental factors described above.

PBSA (2-phenyl-1-H-benzimidazole-5-sulfonic acid) is a heterocyclic sunscreen filter used in the last 20 years in commercial products without any particular drawbacks. It is water-soluble, protects against UVB rays and has a good safety profile. Based on these properties, we recently selected PBSA as a model molecule for sequential modification to obtain potential new sunscreen filters endowed also with other biological properties useful in skin disorders treatment. Completely unattended, the new molecules resulted very potent radical scavenger (useful to counteract UV radiation effects) also endowed with an interesting UV-filter boosting activity when used in combination with conventional UV-sunscreen filters [12].

Inspired by this results, continuing our search for scaffolds for novel multi-active compounds with a good profile of safety, and also to further investigate the above observed effects, we turned our attention to benzothiazoles that are very well represented in several class of drugs such as anti-diabetic [13], Alzheimer [14], antimicrobial [15–21], anthelmintic, anticancer [22–30], analgesic [31,32], anticonvulsant [33–36], trypanocidal [37], antifungal, neuroprotective [35], anti inflammatory [32] and microsomal triglyceride transfer protein (MTP) inhibitors activity [38]. In addition, among the whole class, 2-aryl benzothiazole is the most investigated due to its wide range of synthetic, industrial and pharmaceutical application as amyloid imagining agents [39], schistosomicidial [18], antioxidant, anticancer agents [40].

On the other hand, phenolic compounds are most reactive and important class of natural compounds, because of their biological and pharmacological properties, especially antioxidant activity by H-atom donation or electron transfer [41,42]. Considering that benzothiazoles and phenols exhibit multiple pharmacological properties, including antioxidant effects and skin protection from UVR, their molecular combination could be interesting for the research of new multifunctional compounds.

Taking into consideration the results obtained by us with benzimidazole polyphenols [12], this work focused on the design and synthesis of a series of 2-arylbenzothiazole derivatives which are also isosters of benzimidazole.

By exploiting the structure-activity relationship, an extended investigation on 2-arylbenzothiazole derivatives was developed maintaining the same auxochrome at position 2 and inserting substitutions at the position 6. At this position, we have a proton (-H), a carboxylic acid (-COOH) and a sulfonamide (-SO_2NH_2), these latter are both non-classic isosteres.

2-Phenylbenzothiazole (**4a**) was chosen as reference compound in all the tests performed as it represented the unsubstituted parent compound.

To better discuss the structure-activity relationship, the ten series shown here include both newly synthesized and already known compounds. In order to explore the possibility of a multi-target approach, all synthesized compounds were evaluated for their photoprotective, antioxidant, antifungal and antiproliferative activities.

2. Results and discussion

2.1. Chemistry

In the literature several methods of synthesis of benzothiazoles had been reported such as the condensation of 2-aminothiophenol with substituted nitriles, carboxylic acids, aldehydes, acyl chlorides or esters [43]. After evaluating these methods, we finally turned our attention to simple and effective procedure which involves condensation of 2-aminothiophenol with aldehydes using sodium hydrosulfite as oxidizing agent. Compounds **4b**, **4e**, and **4f** have been also synthesized under free catalyst conditions.

2-Arylbenzothiazoles unsubstituted on the benzothiazole ring (**4a-k**) were synthesized in one-step via condensation of 2-aminothiophenol (**1**) and benzaldehydes (**2a-k**) in ethanol and sodium hydrosulfite as catalyst (Scheme 1). The same reaction, without catalyst, gave a mixture of benzothiazolines (**3a-k**) and benzothiazoles (**4a-k**). Therefore, oxidation of the intermediates **3a-k** was accelerated by $Na_2S_2O_4$.

However, the synthesis of 2,6-disubstituted benzothiazole involved several steps. The initial step was the preparation of intermediates 4-amino-3-mercaptobenzoic acid hydrochloride (**7**) and bis(2-amino-4-benzenesulfonamide)disulfide **(10)** according to a modified literature method [44]. Treatment of 4-aminobenzoic acid with potassium thiocyanate in the presence of bromine in acidic condition at low temperature (0–5 °C) gave 2-aminobenzothiazole-5-carbocylic acid

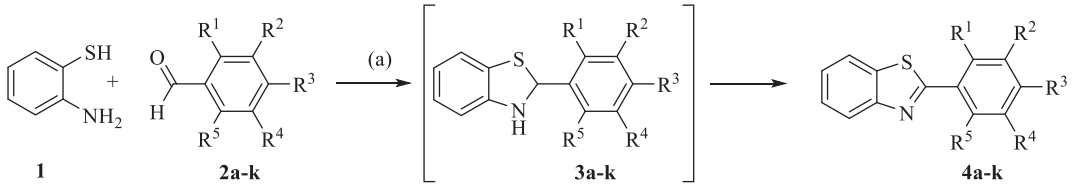

	R^1	R^2	R^3	R^4	R^5
a	H	H	H	H	H
b	OH	H	H	H	H
c	H	OH	H	H	H
d	H	H	OH	H	H
e	H	H	OCH_3	H	H
f	OH	H	OH	H	H
g	OH	H	H	OH	H
h	H	OH	OH	H	H
i	H	OH	OCH_3	H	H
j	H	OH	H	OH	H
k	OH	H	OH	OH	H

Scheme 1. Synthetic route of compounds 4a-k. Reagents and conditions: (a) EtOH, $Na_2S_2O_4$ in H_2O, Reflux.

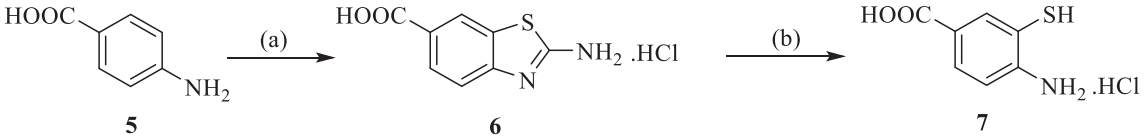

5 6 7

Scheme 2. Synthetic route of 4-amino-3-mercaptobenzoic acid hydrochloride. Reagents and conditions: (a) MeOH, KSCN, Br_2, −5°C, HCl; (b) KOH, Reflux, 35% HCl.

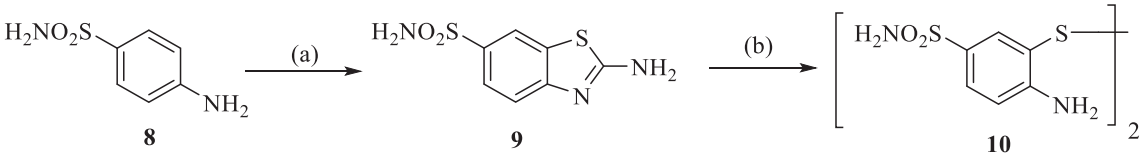

8 9 10

Scheme 3. Synthetic route of bis(2-amino-4-benzenesulfonamide)disulfide. Reagents and conditions: (a) AcOH, KSCN, Br_2 in AcOH, −5°C, 30% NH_3; (b) KOH, Reflux, 35% HCl.

hydrochloride (**6**) which was converted into **7** by alkaline hydrolysis (Scheme 2).

To optimize the synthetic condition for 2-aminobenzothiazole-6-sulfonamide, two solvents were tried: acetic acid and methanol. Acetic acid was found to be the most suitable reaction media giving a high reaction rate and good yield of the product. Treatment of 2-aminobenzothiazole-6-sulfonamide with aqueous potassium hydroxide gave bis(2-amino-4-benzenesulfonamide)disulfide (Scheme 3). Therefore, the thiazole ring was opened but the sulfonamide group did not hydrolyze to a sulfonate.

Subsequently, condensation of **7** or **10** with benzaldehydes (2b-k) yielded to the corresponding benzothiazole compounds (**11b-v**), summarized in Scheme 4. All reactions were conducted in ethanol with catalyst to evaluate the efficiency of sodium hydrosulfite. For all compounds, the best results were obtained in the presence of catalyst. However, among reactions without catalyst, those with bis(2-amino-4-benzenesulfonamide) disulfide gave corresponding 2-arylbenzothiazoles with good yield whereas reaction with 4-amino-3-mercaptobenzoic acid gave the desired product with yield less than 30%.

To better analyze the experimental results, the compounds were divided into ten classes (A-J), which differ from the parent compound for the substitutions on the 2-aryl ring (Table S1). In each class, the compounds present the same substitution on the 2-aryl ring while the substituent at 6 position of the benzothiazole ring change.

2.2. Biological evaluations

2.2.1. Photoprotective activity

Since the Sun Protection Factor (SPF) is related to the UV absorption of the substances, the spectral profile of the synthesized compounds was examined in the first part of this study. Absorption spectra were measured from 290 to 400 nm. The wavelength of maximum absorption (λ_{max}) was closely related to stereo electronic effects, which can be affected by substituents on the 2-aryl or benzothiazole moiety that alter the electron density of compounds. The spectral absorption data of the non-substituted molecules in position 6, dissolved in DMSO, are shown in Fig. 2. The maximum wavelength of **4d** was red-shifted relative to **4c** and can be attributed to the presence of –OH group in para position, which lead the resonance interaction of lone pair of oxygen and π, cloud of 2-aryl and benzothiazole group. This shift increase if -OH is at ortho position (**4b**), due to the presence of the formation of an intramolecular hydrogen bond between nitrogen of benzothiazole and the hydrogen of hydroxy group. Nevertheless, substitution of the para-OH (**4d**) with a para-methoxy (**4e**) does not have significant changes in absorption spectra.

Indeed the absorption spectrum of **4c** is similar to that of 2-arylbenzothiazole (**4a**). This can be explained by the fact that lone electron pair of -OH group in meta position would be delocalized on the 2-aryl ring rather than on the whole entire molecule and, therefore, it has very little effect on the absorption spectrum. However, λ_{max} of **4j** is slightly higher than that of **4c** since both meta positions are occupied,

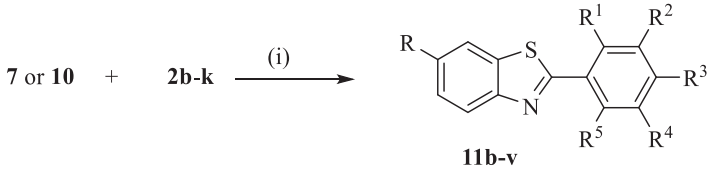

11b-v

	R	R^1	R^2	R^3	R^4	R^5		R	R^1	R^2	R^3	R^4	R^5
b	COOH	OH	H	H	H	H	**m**	SO_2NH_2	OH	H	H	H	H
c	COOH	H	OH	H	H	H	**n**	SO_2NH_2	H	OH	H	H	H
d	COOH	H	H	OH	H	H	**o**	SO_2NH_2	H	H	OH	H	H
e	COOH	H	H	OCH_3	H	H	**p**	SO_2NH_2	H	H	OCH_3	H	H
f	COOH	OH	H	OH	H	H	**q**	SO_2NH_2	OH	H	OH	H	H
g	COOH	OH	H	H	OH	H	**r**	SO_2NH_2	OH	H	H	OH	H
h	COOH	H	OH	OH	H	H	**s**	SO_2NH_2	H	OH	OH	H	H
i	COOH	H	OH	OCH_3	H	H	**t**	SO_2NH_2	H	OH	OCH_3	H	H
j	COOH	H	OH	H	OH	H	**u**	SO_2NH_2	H	OH	H	OH	H
k	COOH	OH	H	OH	OH	H	**v**	SO_2NH_2	OH	H	OH	OH	H

Scheme 4. Synthesis of compounds **11b-v**. Reagents and conditions: (i) EtOH, $Na_2S_2O_4$ in H_2O, Reflux.

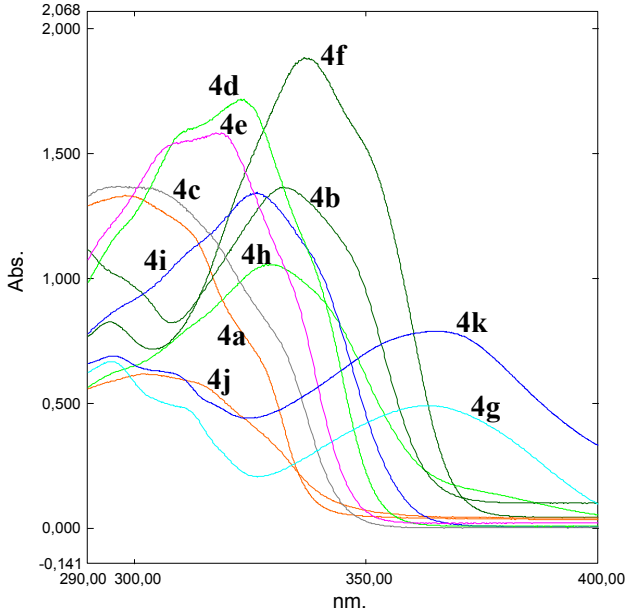

Fig. 2. Spectral profile of benzothiazole derivatives **4a**-**k**.

as confirmed by Joykrishna Dey and al. [45] which demonstrated that red-shift is observed when the number of auxochromic groups increase. The same result is obtained with **4h**, **4i**, and **4g** analogues of **4d**, **4e**, and **4b** respectively, with the second -OH in meta position. The presence of three -OH on the 2-aryl moiety (**4k**) makes the molecule more rigid and promotes the shift at the longest wavelength absorption band compared to the other compounds. Although **4g** has only two hydroxyl groups, its spectrum is similar to that of **4k**, in line with the above mentioned. The presence of an OH in position para has less influence on the shift compared to the other position.

Substitution with an electron withdrawing group (-COOH and $-SO_2NH_2$) at the position 6 of the benzothiazole moiety showed a batochromic shift (Figs. S1 and S2). This long wavelength absorption band is associated with the intramolecular charge transfer transition due to the transfer of the charge between the electron donor group (phenolic group) to the electron-withdrawing of benzothiazole and neighboring carboxylic or sulfonamidic chromophore. The order of λ_{max} along the series is -H $\ll$ $-SO_2NH_2$ $<$ –COOH. Therefore absorption range increase with the trend of the increasing electron-withdrawing ability: this could be mainly due to the significant stabilization of the LUMO leading to a smaller HOMO-LUMO energy space.

In short, beyond the position and the number of -OH on the 2-aryl ring, the presence of an electron-acceptor group at the 6 position of benzothiazole ring, as well as the extent of conjugation, favors the bathochromic shift of the molecule absorption.

Among the proposed *in vitro* methods for the calculation of SPF sun protection, two are the principal: measurement of absorption or the transmission of UV radiation of a thin film of sunscreen agent on the quartz plate or biomimetic membranes and spectrophotometric assay of dilute solutions of sunscreen agent [46–48]. In order to study the synthesized compounds more deeply, both methods were employed. First of all, a pre-screening test was carried out by determination of absorption characteristics of all selected compounds dissolved in DMSO. Then, more promising compounds were introduced in formulation (O/W emulsion) and their transmission spectrum were determined using polymethylmethacrylate (PMMA) plate in order to simulate real human use [49].

2.2.1.1. In vitro studies of dilute solutions of target compounds by spectrophotometry. The photoprotective activity is shown in Table 1. Spectral data of samples were collected in the 290–400 nm range and

Table 1
Values of SPF, UVA-PF, UVA/UVB and λc in DMSO. Each value is the mean of three independent measurements (mean ± SEM).

Classes	Compound	SPF	UVA-PF	UVA/UVB	λc (nm)
	PBSA	3.40 ± 0.17	1.03 ± 0.08	0.29	322
	4a	8.38 ± 0.29	0.13 ± 0.01	1.8	331
	4d	21.86 ± 2.06	1.57 ± 0.02	0.81	353
A	**11d**	6.19 ± 0.98	2.23 ± 0.08	0.81	353
	11o	19.41 ± 1.75	2.35 ± 0.10	0.32	350
	4e	14.23 ± 1.43	1.30 ± 0.04	0.1	335
B	**11e**	6.54 ± 0.87	1.88 ± 0.12	0.65	349
	11p	8.91 ± 0.45	1.80 ± 0.09	0.45	347
	4c	10.05 ± 0.11	1.18 ± 0.07	0.13	335
C	**11c**	8.84 ± 0.64	1.71 ± 0.02	0.36	346
	11n	9.42 ± 0.06	1.46 ± 0.05	0.18	340
	4b	7.56 ± 0.59	2.57 ± 0.06	0.86	355
D	**11b**	18.03 ± 1.15	4.09 ± 0.14	0.62	358
	11 m	6.59 ± 0.83	3.45 ± 0.22	0.77	360
	4f	6.62 ± 0.07	3.34 ± 0.13	1.62	356
E	**11f**	3.43 ± 0.49	4.62 ± 0.05	1.61	370
	11q	3.85 ± 0.31	4.41 ± 0.11	1.63	364
	4h	5.51 ± 0.96	2.33 ± 0.16	0.9	358
F	**11h**	7.42 ± 0.13	7.35 ± 0.41	1.74	367
	11s	5.39 ± 0.09	4.71 ± 0.08	1.40	365
	4i	9,13 ± 0.34	5.94 ± 0.15	0.42	350
G	**11i**	17.33 ± 1.45	5.95 ± 0.26	1.02	361
	11t	11.87 ± 0.07	5.80 ± 0.33	0.96	380
	4g	2.82 ± 0.49	2.50 ± 0.17	0.66	381
H	**11g**	7.34 ± 0.49	3.32 ± 0.24	0.40	384
	11r	5.47 ± 0.07	2.76 ± 0.01	0.40	382
	4j	3.38 ± 0.16	1.52 ± 0.09	0.45	345
I	**11j**	4.45 ± 0.23	1.57 ± 0.07	0.45	353
	11u	3.06 ± 0.06	1.72 ± 0.02	0.95	380
	4k	3.87 ± 0.012	4.71 ± 0.08	0.86	385
J	**11k**	5.16 ± 0.33	7.50 ± 0.42	1.25	389
	11v	3.65 ± 0.15	4.20 ± 0.19	1.34	384

the data were elaborated by the calculator software [50]. The software consent to evaluate COLIPA (The European Cosmetic and Perfumery Association) – SPF, COLIPA – UVA-PF, critical wavelength value (λc) (see Eq. (3), Eq. (4) and Eq. (5)) and UVA/UVB ratio as preliminary theoretical data.

All the synthesized compounds, in general, showed a significant photoprotective activity as compared to photoprotective activity of the lead compound PBSA. Photoprotective activity of the sunscreen against UVB is reported as SPF value. Thereby, among all classes of compounds having a single substituent on the 2-aryl ring, those without substituent at the 6-position of the benzothiazole moiety exhibited good photoprotective profile, followed by compounds having $-SO_2NH_2$, and finally compounds having -COOH. Only in class **D**, compound bearing -COOH showed the best SPF value.

Moreover, it was evident that the substitution of benzothiazole ring by COOH and SO_2NH_2 had no significant effect on sun protection. Taking all together, we can summarize that the presence of a hydrogen atom in 6 position of benzothiazole ring increases SPF value, therefore the SAR order was -H $>$ $-SO_2NH_2$ $>$ -COOH. On the contrary, among the compounds having more than one substituent on the 2-aryl ring, those bearing -COOH group showed the best UVB profile except the compound **11f**. However, the order of SPF values according to the substitution on the 2-aryl ring was the following: para $>$ meta $>$ ortho for compounds having -H or $-SO_2NH_2$ at 6 position of benzothiazole moiety, while compounds with -COOH gave the following order: ortho $>$ meta $>$ para. Compounds of class **B** (para-methoxy substituted on the 2-aryl ring) showed lower value than compounds of class **A**, indicating that para-hydroxy group is better than para-methoxy one, except compound **11d** which showed SPF value slightly lower than that of **11e**.

The introduction of an -OH in position ortho or meta of compounds of class **A** to obtain compounds of classes **E** and **F** respectively, yield to a decrease of SPF values. In the same way, introduction of -OH in meta

position of compounds of class **D** (ortho-OH) and class **C** (meta-OH) gave respectively compounds of classes **H** (two -OH in position 2 and 5) and **I** (two -OH in position 3 and 5) with lower SPF. Interestingly, compounds of class **J** with three -OH on the 2-aryl ring showed SPF values similar to those with two -OH. This means that the SPF factor not only depends on the number of -OH on the 2-aryl ring but also on their position. Interestingly, replacing para-hydroxy with para-methoxy (class **F** to **G**) the SPF values increase. Nevertheless, this result is contrary to that previously described (class **A** to **B**). The best SPF value is exhibited by compound **4d** bearing an -OH in para position of 2-aryl ring. Protection offered by a sunscreen product against chronic damages (i.e. tumor formation) induced by UVA rays is indicated by UVA-PF value, which is considered sufficient for protection against UVA by European regulation if its value results ≥ 1/3 of SPF. Compounds of the same class presented similar UVA-PF values despite they differ in substitution at position 6. Compounds **11 h** of class **F** and **11 k** of class **J**, characterized both by the presence of -OH in meta and para-position of the phenyl ring, are the best candidate for UVA protection (with UVA-PF ≈ 7), followed by compounds of class **G** (3-OH, 4-OMe). Thus, the effect of the electron donor group (hydroxyl or methoxyl) in the meta and para position of the 2-aryl ring appears to be important for protection against UVA.

Critical wavelength (λc) is the parameter that provides information on the broad spectrum of UV-filter. It is classified in five numerical categories: 0 (λc < 325 nm), 1 (325 ≤ λc ≤ 335), 2 (335 ≤ λc ≤ 350), 3 (350 ≤ λc < 3 7 0) and 4 (λc ≥ 370). FDA considers that the broad-spectrum sunscreen products should have a λc ≥ 370 nm [51]. Under that classification, compounds of classes **H** and **J** have fallen into category "4″, as well as compounds **11f** (class **E**), **11t** (class **G**) and **11u** (class **I**). All synthesized compounds showed λc > PBSA. Thus, very interestingly, compounds of classes **H**, **J** and compounds **11f**, **11t** and **11u** can be considered potential candidate for broad-spectrum filters.

Finally, we also determined the UVA/UVB absorbance ratio, which is an important parameter to get information on the absorbance through the entire UV spectrum. According to the latest EU recommendation and PBSA data (the UVA/UVB ratio should be at least 1/3), all synthesized compounds have good UVA/UVB values, apart from **11o**, **4e**, **4c** and **11n**.

2.2.1.2. In vitro sun protection factor of the cosmetic formulation. On the basis of the results obtained in solution, it was decided to continue the investigation on compounds of class **A** and **J**, representative of derivatives with the best UVB profile and broad spectrum, respectively. The 6 molecules synthesized and selected were then inserted at the concentration of 1% in a conventional cosmetic formulation O/W in order to deepen their UV-filter activity. The modified *in vitro* method of Diffey and Robson [46], based on the measurement of transmission of ultraviolet radiation on the PMMA plate, was used. Data of the SPF, UVA-PF, UVA/UVB and λc parameters are shown in Table 2.

Table 2
Photoprotection results of 1% benzothiazole selected derivatives in O/W formulations. Each value is the mean of three independent measurements (mean ± SEM).

Classes	O/W Formulation	SPF	UVA-PF	UVA/UVB	λc (nm)
	PBSA	3.02 ± 0.89	1.04 ± 0.06	0.26	333
	4d	3.2 ± 0.21	1.20 ± 0.11	0.63	350
A	**11d**	1.57 ± 0.09	1.79 ± 0.10	1.12	353
	11o	1.99 ± 0.18	3.59 ± 0.24	1.35	351
	4k	3.66 ± 0.29	3.24 ± 0.26	0.81	385
J	**11**	3.91 ± 0.24	3.33 ± 0.11	0.86	388
	11v	2.82 ± 0.19	3.26 ± 0.25	1.15	385

Table 3
Evaluation of photostability of 1% benzothiazole selected formulations. Each value is the mean of three independent measurements (mean ± SEM).

Classes	Compound	$\%SPF_{eff.}$	$\%UVA\text{-}PF_{eff.}$
	4d	94.06 ± 0.04	98.07 ± 0.23
A	**11d**	97.45 ± 0.08	99.85 ± 0.35
	11o	95.21 ± 0.73	100.0 ± 0.04
	4k	94.28 ± 3.07	98.64 ± 2.09
J	**11k**	97.37 ± 0.22	99.35 ± 0.17
	11v	98.44 ± 1.55	99.76 ± 2.08

Taking into consideration the spectral data of diluted solutions and cosmetic formulations, we can affirm that the structure-activity relationship is in principle maintained in both cases. Compound **11 k**, characterized by the presence of three hydroxy groups in position 2,4,5 of the 2-aryl ring, showed the best SPF value (SPF = 3.91). This value is significant since the formulation contains only 1% of active ingredient. Compounds **4 k**, **11 k**, and **11v** of class **J** have confirmed their profile and are therefore potential compounds for broad-spectrum UV filters. *In vitro* data of the formulations indicated that the presence of auxocromes influences the photoprotective profile..

2.2.1.3. Photostability study. Photostability of selected compounds was evaluated using one of the criteria developed by Garoli at al. [52], based on the measurement of SPF before and after exposition. The loss of sunscreen protection after exposure to sunlight is expressed as the residual effectiveness after exposure (%). The *in vitro* % $SPF_{eff.}$ and % $UVA\text{-}PF_{eff.}$ of compounds are calculated according to Eqs. (6) and (7) respectively and are reported in Table 3. A sunscreen was considered photostable if its residual percentage is greater than or equal to 80%. From the results obtained, % $SPF_{eff.}$ and % $UVA\text{-}PF_{eff.}$ values of compounds ranged from 94.06 to 100%. Therefore, these compounds are considered photostable with a degradation rate less than 6%. Interestingly, the substitution of the benzothiazole ring in position 6 with -COOH or $-SO_2NH_2$ increases the photostability of the compounds.

2.2.2. Antioxidant activity

The synthesized compounds were then tested *in vitro* to evaluate the antioxidant activity which, if present, is very important and synergistic with the SPF described above in reducing UV-induced ROS damages. The method employed were DPPH and FRAP assays (Table 4).

2.2.2.1. DPPH radical scavenging activities. To better understand the results of the DPPH test, we first evaluated the percentage of inhibition of the DPPH radical of synthesized compounds at the same concentration, namely 1 mg/mL. Compounds of classes **F** (3,4-dihydroxyaryl) and **H** (2,5-dihydroxyaryl) have a percentage of inhibition close to 100%. However, the substitution of -OH with $-OCH_3$ to obtain class **G** (3-hydroxy, 4-methoxy), lead to a decreases of the percentage of inhibition. Compounds of class **A**, with -OH in para position on the 2-aryl ring, did not exhibit any particular activity with respect to the radical under consideration. In this case, replacing -OH with $-OCH_3$ to obtain class **B** compounds lead to a considerably increase of the percentage of inhibition compounds **4e** and **11e** In addition, among compounds of class **D**, only **11m** with -OH in ortho position of 2-aryl ring and SO_2NH_2 in 6 position of the benzothiazole ring displayed a good inhibition. Alike, for compounds of class **C** (meta-hydroxy), only compound **11c** with COOH in 6-position on benzothiazole ring has good inhibition. The introduction of methoxy group at position 4 of the 2-aryl ring (compounds of class **G**) drastically reduced the activity in comparison to compounds of class **F**, due to the lack of stabilization.

Based on this first screening, only compounds with good inhibition (% ≥ 50) were further investigated for the determination of IC_{50} values. The results are expressed in μg/mL (Table 4). Structure-activity relationship analysis indicated that various factors such as the nature of

Table 4
Antioxidant activity of benzothiazole derivatives. Each value is the mean of three independent measurements (mean ± SEM).

Classes	Compound	DPPH %Inhibition	DPPH IC_{50} (μg/ml)	FRAP μmolT/g
	4a	43.6 ± 0.11	974.49 ± 4.78	167.01 ± 3.34
	4d	11.60 ± 0.32	–	123.00 ± 5.92
A	**11d**	30.75 ± 0.89	–	402.17 ± 1.95
	11o	31.22 ± 0.45	–	65.60 ± 1.18
	4e	45.27 ± 0.61	–	206.88 ± 6.64
B	**11e**	71.70 ± 0.58	322.70 ± 6.29	173.83 ± 5.05
	11p	15.48 ± 0.33	–	90.95 ± 3.64
	4c	16.27 ± 0.06	–	48.61 ± 0.40
C	**11c**	94.64 ± 1.22	28.97 ± 0.56	2045.37 ± 18.68
	11n	22.73 ± 0.69	–	17.36 ± 0.81
	4b	30.72 ± 0.47	–	264.75 ± 5.84
D	**11b**	18.00 ± 0.36	–	20.60 ± 0.85
	11m	58.22 ± 0.87	–	197.80 ± 5.07
	4f	72.83 ± 0.58	822.63 ± 8.16	187.64 ± 5.15
E	**11f**	22.37 ± 0.52	–	50.32 ± 1.54
	11q	23.89 ± 0.48	–	91.31 ± 3.25
	4h	84.65 ± 0.93	7.2 ± 0.11	6021.15 ± 25.84
F	**11h**	94.74 ± 0.66	11.29 ± 0.07	7402.73 ± 22.78
	11s	94.36 ± 0.82	7.96 ± 0.55	5273.01 ± 15.01
	4i	65.00 ± 0.31	561.62 ± 18.13	3247.66 ± 56.72
G	**11i**	28.02 ± 0.87	–	712.52 ± 10.75
	11t	10.98 ± 0.11	–	65.39 ± 0.35
	4g	94.32 ± 1.15	6.42 ± 0.28	6268.43 ± 25.16
H	**11g**	96.41 ± 0.89	7.61 ± 0.28	7321.64 ± 34.73
	11r	96.23 ± 0.77	9.09 ± 0.24	7115.91 ± 14.46
	4j	77.5 ± 4.76	159.55 ± 6.20	273.49 ± 15.38
I	**11j**	57.9 ± 0.82	–	175.98 ± 1.78
	11u	19.93 ± 1.54	–	73.33 ± 1.42
	4k	23.78 ± 0.82	–	4876.44 ± 34.54
J	**11k**	72.73 ± 3.67	43.01 ± 2.93	1960.24 ± 18.43
	11v	53.20 ± 0.95	186.89 ± 5.46	513.04 ± 2.66

substituents in position 6 on benzothiazole ring, the number and also the position of the electron donor group (-OH and -OCH_3) on the 2-aryl ring are very important for the radical scavenging activity. All compounds of class **F** and **H** especially those without electron withdrawing group on the benzothiazole ring (**4h** and **4g**) showed good inhibition, with IC_{50} values between 6.42 and 11.29 μg/mL, respectively. This could be due to the fact that, polyphenols having two -OH groups in the 2,5- and 3,4-positions react twice with DPPH radical to form a very stable conjugated diketone structure, further stabilized the hydrogen bonds between two hydroxy for the 3,4-dihydroxy compounds and between one hydroxy and nitrogen of the benzothiazole ring for the 2,5-dihydroxy compounds. Nevertheless, introduction of methoxy group at position 4 of the 2-aryl ring (compounds of class **G**) drastically reduced the activity in comparison to compounds of class **F** (in term of percentage of inhibition), due to the lack of stabilization above mentioned. Surprisingly, compound **11c** with meta-hydroxy group displayed good activity, while compound 3,5-dihydroxysubstituted on 2-aryl ring have no activity. In addition, compounds of class **J**, although having three -OH group, are less active than their parent compounds (compounds of class **H**). This could be explained by the fact that the presence of the third -OH prevents the resonance.

2.2.2.2. Ferric reducing potential. Similar to DPPH results, the molecules with a better antioxidant profile are those of classes **F** and **H** which bear two hydroxy groups respectively at positions 3, 4 and 2, 5- of the 2-aryl ring. The compounds of classes **A** and **D**, having para and ortho hydroxy on the 2-aryl ring respectively, have moderate values. Among compounds of class **C**, **11c** bearing -COOH on the benzothiazole ring have a good activity (2045.37 ± 18.68 μmolT/g), instead both **4c** and **11n** have very low values (48.61 ± 0.40 and 17.36 ± 0.81μmolT/g respectively). The substitution of the hydroxyl group in para (class **A**) with a methoxyl (class **B**) did not lead to significant changes in the activity, except for the compound 11d, whose correspondent 11e has more than halved activity. Instead the replacement of the para methoxy group (class **G**) with an hydroxyl group (Class **F**) led to a significant increase in activity, indicating that para methoxy substitution is not suitable for this activity.

In summary, considering the above mentioned results, in DPPH and FRAP assays, molecules with better antioxidant profile are compounds of classes **F** and **H**, which bear two hydroxy groups at positions 3, 4 and 2, 5- of the 2-aryl ring.

2.2.3. Antifungal activity

2.2.3.1. Antidermatophytic activity. All synthesized compounds were investigated to determine their antifungal activity against five dermatophytes responsible for the most common dermatomycoses: *Microsporum gypseum*, *Microsporum canis*, *Trichophyton mentagrophytes*, *Trichophyton tonsurans* and *Epidermophyton floccosum*. Inhibition of dermatophytes was evaluated by inhibition growth method in Sabouraud Dextrose Agar (SDA), using DMSO as a solvent. All compounds were tested at a concentration of 100 μg/ml (Tables S2). Compound **4h** showed the highest antifungal activity. It is active against all five dermatophytes, in particular against *M. gypseum, T. tonsurans* and *E. floccosum* with a percentage of inhibition close to 100%. Significant activity was observed for compounds **4f** and **4g** against *M. gypseum* and *E. floccosum*. Compound **4c** and **4j** showed good activity against *Microsporum gypseum* and *Epidermophyton floccosum* respectively. In general it can be stated that compounds substituted in position 6 of the benzothiazole ring showed a reduced activity, thus suggesting that electron withdrawing substituent decrease the antifungal activity.

In addition compound **4h,** identified as the most active in the previous screening, was also evaluated for its potency against *M. gypseum, T. tonsurans* and *E. floccosum* as reported in Table 5.

2.2.3.2. Anti-Candida activity. The antifungal activity of the synthesized compounds was also determined against Candida albicans (ATCC 10231). Minimal inhibitory concentration (MIC) of the

Table 5
IC_{50} values of **4h** benzothiazole derivate and Fluconazole. Each value is the mean of three measurements (mean ± SEM).

	IC_{50} μg/ml		
	M. gypseum	*T. tonsurans*	*E. floccosum*
4h	26.95 ± 1.04	43.31 ± 1.85	11.63 ± 0.24
Fluconazole	18.5 ± 1.23	19.41 ± 0.87	0.08 ± 0.005

Table 6
Anti-*Candida albicans* activities of benzothiazole derivatives. The average values were taken as the MICs.

Compound	MIC μg · ml $^{-1}$	
	24h	**48h**
4f	4	32
4h	32	32
4k	8	128
11k	64	–
11v	128	–
Fluconazole	0.5	–

synthesized agents was determined by broth microdilution method using RPMI (Roswell Park Memorial Institute) 1640 + MOPS (3-(*N*-Morpholino)propanesulfonic acid sodium salt). The concentration of the tested compounds ranged from 0.25 μg·mL^{-1} to 128 μg·mL^{-1}. The growth in the 96-well microdilution plate was observed visually for turbidity and inhibition was determined by the absence of growth. MIC was determined by the lowest concentration of the sample that prevented the development of turbidity. The results, shown in Table 6, are representative of 24 and 48 h of incubation arranged in triplicate (only active compounds against *Candida albicans* were shown). Fluconazole was used as referenced compound. Derivative **4h**, **4f**, **4k**, showed good activity. In particular, compounds **4f** and **4k** characterized respectively by the presence of -OH groups in positions 2, 4 and 2, 4, 5 of the 2-aryl ring and no functional group on the benzothiazole ring are more effective with a range of MIC of 4–8 μg/mL at 24 h.

2.2.4. Antiproliferative activity

Antiproliferative activities of target compounds against human T cell leukemia cell line (CEM), human cervix carcinoma cells (HeLa), human pancreas carcinoma cells (Mia Paca-2) and human melanoma cells (SK-Mel 5) were evaluated *in vitro* and summarized in Table 7. The results were expressed as IC_{50} values in μM and normal kidney epithelial cells (HEK 293) were chosen as control of cytoxicity and/or selectivity.

Among the tested compounds, **4e**, **11n** and **11o** were the most potent against Mia Paca-2 cells with IC_{50} values of 6.6, 5.5 and 6.5 μM respectively, but inactive against HeLa and CEM cells (IC_{50} > 50 μM). However, **4e** also displayed good activity against SK-Mel5 cells while **11n** and **11o** were moderately active. Compounds **4g** and **4h** exhibited good antiproliferative activity against CEM and SK-Mel 5 cells with IC_{50} < 10 μM and a moderate activity against HeLa and Mia Paca-2 (IC_{50} > 20 μM). **4k** showed the best activity against SK-Mel 5 and it also displayed good inhibitory activity against CEM.

Interestingly, substitution of the para hydroxyl group of compound **4d** with a methoxy group led to compound **4e** endowed with increased antiproliferative activity against Mia Paca-2 cell (52 to 6.6 μM respectively). Similarly, the introduction of -SO_2NH_2 at the 6-position on the benzothiazole ring (**11o**) increase potency. Curiously, in this case, substitution by para-methoxy has the same effect on Mia Paca-2 cell as substitution by -SO_2NH_2 in position 6 on benzothiazole, therefore activity of **4e** is similar to **11o**. The shift of the hydroxyl group along 2-aryl group did not have significant effect on the activity, whereas the introduction of a second or third hydroxyl group (compound **4g**, **4h**, and **4k**) led to an increase in the antiproliferative activity on the CEM and SK-Mel 5 cells.

After introduction of the -SO_2NH_2 group into the benzothiazole skeleton of **4c** to obtain **11n**, an increase in activity against Mia Paca-2 cells was observed but activity against CEM, HeLa and SK-Mel 5 cells decreased. Apart from **4c** and **4d**, the introduction of -SO_2NH_2 into the backbone reduces the activity against Mia Paca-2 cells. All tested compounds showed low antiproliferative activity towards HeLa cell line, except compound **4h** with an inhibition activity less than 30 μM. To our surprise, replacement of the -SO_2NH_2 with -COOH led to almost total loss of activity.

Based on cytotoxicity screening, all unsubstituted compounds on the benzothiazole ring were cytotoxic to normal HEK 293 except compound **4e** and **4i** with para-methoxy group on 2-aryl ring, suggesting the importance of para-methoxy for antiproliferative activity. As well as **4b** and **4k** bearing respectively one and three hydroxy group was not cytotoxic. However electron-withdrawing group -SO_2NH_2 on the benzothiazole ring decreases the cytotoxicity of the target compound except compound **11o** and **11s** characterized by the the presence of para-hydroxy group on 2-aryl ring. Compounds bearing -COOH on the benzothiazole ring (**11a-11k)** were inactive against both normal and cancer cells.

The Selectivity Index (SI) was determined by comparing the IC_{50} values (μM) obtained on the healthy cells (HEK 293) with that obtained on cancer cells (CEM, HeLa, Mia-Paca-2 and SK-Mel 5). From the results presented in Table 7, we observed that compounds **4e**, **11n** and **11o** were respectively 15, 18 and 5 fold more selective toward Mia-Paca-2 cells, while compounds **4g** and **4k** were approximately 6 fold more selective for CEM cells. In addition, compounds **4e**, **4i** and **4k** showed selectivity for SK-Mel 5 cells. Compounds **4k** were 25 fold more selective for SK-Mel 5 cells that could be due to the presence of three hydroxy groups on the 2-aryl ring. SI values indicated as the best compounds the derivative **11n**, selective towards the Mia-Paca-2, the selective derivative **4e** for both the Mia-paca-2 and for the SK-Mel5 and the **4g** and **4k** selective derivatives for the CEM and the SK-Mel5. The particularity of these last two compounds is the presence of -OH in position 2 and 5 on the 2-aryl ring. Therefore, these two positions are very important for the activity sought.

2.2.5. Benzothiazole derivatives block hERG potassium channels expressed in HEK293 cells

In order to have an idea of the possible mechanism of compounds presenting a good antiproliferative profile, we studied the effect of these derivatives on the modulation of human ether-a-go-go related gene (hERG) current. hERG is a gene (KCNH2) that encodes for a protein highly selective for potassium channel (K_v11.1). These protein channels are widely expressed, mainly in the cardiac tissues, neuronal tissues, brain, adrenal gland, thymus, retina and in some cancer cells [53]. Indeed, the ion channels are transmembrane proteins that regulate the flow of ions through biological membranes. In particular, potassium channels represent the most diverse group of ion channels and play an important role in several functions such as muscle excitation, regulation of blood pressure [54], proliferation of several types of cancer, such as prostate, colon, and glioma [55–57]. It has been shown that, hERG potassium channels are overexpressed in many types of human cancers as well as in primary human cancers [58,59]. In addition, it was shown that over-expression of hERG channels in HEK-293 cells greatly increased the proliferation, tumor cell invasion and metastasis. The blockade or inhibition of hERG in these cells induced both antiproliferative and antimigratory effect [60,61]. Thus the interest in the study of hERG channels has increased exponentially, mainly because of its involvement in many cellular events such as repolarization and proliferation of cells [62]. Therefore, given their multifunction, these channels are potential therapeutic targets for cancer treatment by

Table 7
Inhibitory effects of benzothiazole derivatives on the proliferation of CEM, HeLa, Mia Paca-2 and SK-Mel 5. Each value is the mean of three independent measurements (mean ± SEM). SI = IC_{50} of pure compound in a normal cell line/IC_{50} of the same pure compound in cancer cell line.

		IC_{50} μM					SI			
Classes	Compound	CEM	HeLa	Mia-Paca-2	SK-Mel5	HEK 293	CEM	HeLa	Mia-Paca-2	SK-Mel5
Reference	**4a**	> 100	100	≥100	82 ± 23	> 100	–	–	–	1.22
	4d	52 ± 0.0	46 ± 10	52 ± 10	51 ± 3	50 ± 2	0.96	1.09	0.96	0.98
A	**11d**	77 ± 32	> 100	> 100	> 100	> 100	1.30	–	–	–
	11o	64 ± 24	67 ± 25	6.5 ± 0.5	33 ± 6	32 ± 4	0.50	0.48	4.92	0.97
	4e	> 100	> 100	6.6 ± 3.3	14 ± 2	> 100	–	–	15.15	7.14
B	**11e**	> 100	> 100	> 100	> 100	> 100	–	–	–	–
	11p	> 100	> 100	47 ± 16	> 100	> 100	–	–	2.13	–
	4c	38 ± 2	44 ± 8	62 ± 14	17 ± 10	46 ± 2	1.21	1.05	0.74	2.71
C	**11c**	> 100	> 100	72 ± 39	> 100	> 100	–	–	1.39	–
	11n	58 ± 19	77 ± 12	5.5 ± 3.1	43 ± 1	≥100	1.72	1.30	18.18	2.33
	4b	63 ± 16	93 ± 10	> 100	34 ± 10	> 100	1.59	1.08	–	2.94
D	**11b**	> 100	> 100	> 100	≥100	> 100	–	–	–	–
	11m	> 100	≥100	> 100	≥100	> 100	–	–	–	–
	4f	52 ± 0.0	46 ± 10	52 ± 10	51 ± 3	50 ± 2	0.96	1.09	0.96	0.98
E	**11f**	> 100	> 100	≥100	> 100	> 100	–	–	–	–
	11q	> 100	> 100	≥100	> 100	73 ± 38	–	–	–	–
	4h	8.2 ± 5.7	29 ± 16	40 ± 21	5.4 ± 0.3	15 ± 4	1.83	0.52	0.38	2.78
F	**11h**	> 100	> 100	> 100	> 100	> 100	–	–	–	–
	11s	19 ± 5	45 ± 9	41 ± 22	25 ± 2	14 ± 5	0.74	0.31	0.34	0.56
	4i	51 ± 15	≥100	> 100	25 ± 3	≥100	1.96	–	–	4.00
G	**11i**	> 100	> 100	80 ± 25	95 ± 7	> 100	–	–	1.25	1.05
	11t	59 ± 13	80 ± 29	≥100	> 100	≥100	1.69	1.25	–	–
	4g	2.0 ± 1.6	74 ± 29	38 ± 3	5.3 ± 0.5	13 ± 5	6.50	0.18	0.34	2.45
H	**11g**	> 100	> 100	66 ± 35	> 100	> 100	–	–	1.52	–
	11r	22 ± 6	90 ± 14	72 ± 21	> 100	62 ± 17	2.82	0.69	0.86	–
	4j	32 ± 5	38 ± 6	52 ± 4	28 ± 2	33 ± 9	1.03	0.87	0.63	1.18
I	**11j**	> 100	> 100	≥100	> 100	> 100	–	–	–	–
	11u	89 ± 15	> 100	≥100	74 ± 6	≥100	1.12	–	–	1.35
	4k	18 ± 2	> 100	> 100	4.0 ± 0.2	> 100	5.56	–	–	25.00
J	**11k**	91 ± 13	> 100	> 100	64 ± 26	> 100	1.10	–	–	1.56
	11v	> 100	> 100	> 100	> 100	> 100	–	–	–	–

application of hERG channel blocking.

One of the most accurate methods for determining the potency of a compound in K^+ channel inhibition is patch-clamp electrophysiology. In this work we focused on the QPatch automated patch clamp system to evaluate the blockade of hERG potassium channels expressed in HEK293 cells. Three different concentrations (0.1, 1 and 10 μM) of benzothiazole derivatives were tested and summarized in Table 8. E-4031 (methanesulfonanilide class III antiarrhythmic agent) is the reference compound for this assay. The percent inhibition of the peak tail current was measured, the concentration of drugs needed to yield a 50% blockade of the hERG current (IC_{50}) was obtained by fitting the data to a Hill equation (Eq. (10)).

At the higher tested concentration (10 μM) **4g** reduced hERG current amplitude to 60.32 ± 2.43 %with IC_{50} equal to 4,79 μM, while **4e**, **11c** and **11d** have an inhibition less than 50%. As compared to the reference compound, **4g** is a potential candidate for blocking HERG potassium channels.

Table 8
Inhibition of hERG channels by benzothiazole derivatives tested at 10 μM. Each value is the mean of three independent measurements (mean ± SEM).

Compound	hERG activity channels	
	pIC_{50}	% Inhibition
4e	< 5	12.09 ± 5.05
4 g	5.32 ± 0.04	60.32 ± 2.43
4 k	< 5	41.17 ± 2.94
11c	< 5	20.73 ± 1.79
11d	< 5	8.07 ± 4.08
E-4031	7.55 ± 0.08	96.32 ± 0.9

3. Experimental section

3.1. General

Reagents and solvents were purchased from Sigma-Aldrich and Carlo Erba Reagenti (Italia) and without further purification. Analytical TLC was performed on silica gel plates (Macherey-Nagel Poligram SIL G/UV254 0.20 mm) and visualized by exposure to ultraviolet light (254 nm) and /or used 1% solution of $KMnO_4$. Column chromatography was performed using silica gel Macherey-Nagel 60 M 230,400 mesh. ^1H NMR and ^{13}C NMR were registered with Varian spectrometers at 200 MHz and 400 MHz at room temperature. Chemical shifts are measured with respect to tetramethylsilane and relative to residual solvent peaks as an internal standard set to D_2O and $(CD_3)_2SO$. The following abbreviations are used to indicate signal multiplicity: s (singlet), d (doublet), t (triplet), q (quartet), m (multiplet), brs (broad singlet) and dd (doublet of doublets). Molecular weights of the compounds were determined by ESI (Micromass ZMD 2000), and the values are expressed as $[MH]^+$. UV spectrophotometric analyses were carried out on a UV–VIS spectrophotometer (Shimadzu UV-2600). IR analyses were performed on FT-IR spectrometer Spectrum 100 (Perkin Elmer precisely).

3.2. Chemistry

3.2.1. General method for the synthesis of 2-Arylbenzothiazoles unsubstituted on the benzothiazole ring

To a solution of 2-aminothiophenol (0.4 g, 3.2 mmol) and aldehyde (3.2 mmol) in ethanol (3.5 mL) at room temperature was added solution of sodium hydrosulfite (2 eq. in 3 mL H_2O). The mixture was heated at reflux for 12 h. After cooling to room temperature, the solution was concentrated in vacuo. The residue was treated with HCl 2 N

(15 mL) and filtered to obtain the crude solid, which was recrystallized from appropriate solvent. Compounds **4b**, **4e** and **4f** were synthesized with and without catalyst following the same procedure described above.

*3.2.1.1. 2-phenylbenzo[d]thiazole **(4a)***. Yield 60%; white solid; m.p. 98–99 °C; UV λmax 298.4 nm. IR (KBr) cm^{-1}: 3446.7, 1589.75, 1474.3, 1316.4, 1217.2, 756.9. ^{1}H NMR (400 MHz, DMSO-d_6): δ (ppm) 8.10 (d, J = 8 Hz, 1H, BTZ), 8.01 (d, J = 8 Hz, 1H, BTZ), 7.74 (m, 2H, Ar), 7.33 (m, 5H, 2H BTZ, 3H Ar). ^{13}C NMR (400 MHz, DMSO-d_6): δ (pmm) 169.45, 154.4, 143.65, 133.32, 131.87, 130.32, 129.00, 126.76, 124.54, 123.67, 120.09. ESI-M $[M+H]^+$: calcd for $C_{13}H_9NS$, 211.28; found 212.20.

*3.2.1.2. 2-(2-hydroxyphenyl)benzo[d]thiazole **(4b)***. Yield 80%; yellow solid; m.p. 125–126.4 °C; UV λmax 331.4 nm. IR (KBr) cm^{-1}: 3000.5, 1589.1, 1479.8, 1315.2, 1214.4, 724.7. ^{1}H NMR (400 MHz, DMSO-d_6): δ (ppm) 11.65 (brs, 1H, OH), 8.21–8.18 (2H, m, BTZ), 8.07 (d, J = 8 Hz, 1H, Ar), 7.58 (t, 1H, BTZ), 7.39 (m, 2H, 1H BTZ, 1H Ar), 7.15 (d, J = 8.0 Hz, 1H, Ar), 7.01 (t, J = 7.2 Hz, 1H, Ar). ^{13}C NMR (400 MHz, DMSO-d_6): δ (pmm) 165.59,156.65, 151.83, 134.68, 132.95, 128.95, 126.94, 125.56, 122.54, 122.45, 120.25, 118.76, 117.38. ESI-MS $[M+H]^+$: calcd for $C_{13}H_9NOS$, 227.28; found 228.17.

*3.2.1.3. 2-(3-hydroxyphenyl)benzo[d]thiazole **(4c)***. Yield 71%; yellow solid; m.p. 158–159 °C; UV λmax 299.4 nm. IR (KBr) cm^{-1}: 3251.3, 1598.0, 1453.6, 1317.1, 1231.3, 759.0. ^{1}H NMR (400 MHz, DMSO-d_6): δ (ppm) 9.93(brs, 1H, OH), 8.19 (d, J = 8.0 Hz, 1H, BTZ), 8.08 (d, J = 8.0 Hz, 1H, BTZ), 7.60–7.39 (m, 3H BTZ, 2H Ar), 6.99 (dd, J = 8.4 Hz, J = 1.6HZ, 1H, Ar). ^{13}C NMR (400 MHz, DMSO-d_6): δ (pmm) 167.79, 158.42, 153.94, 134.80, 134.45, 131.03, 127.09, 125.97, 123.30, 122.79, 118.99, 118.54, 113.83. ESI-MS $[M+H]^+$: calcd for $C_{13}H_9NOS$, 227.28; found 228.30.

*3.2.1.4. 2-(4-hydroxyphenyl)-benzo[d]thiazole **(4d)***. Yield 78%; yellow solid; m.p. 224–225 °C; UV λmax 323.5 nm. IR (KBr) cm^{-1}: 3200.5, 1603.5, 1424.7, 1283.5, 754.4. ^{1}H NMR (400 MHz, DMSO-d_6): δ (ppm) 10.22 (brs, 1H, OH), 8.08 (d, J = 8.0 Hz, 1H, BTZ), 7.98–7.96 (m, 3H, BTZ), 7.56–7.38 (m, 2H, Ar), 6.91 (d, J = 8.4 Hz, 2H, Ar). ^{13}C NMR (400 MHz, DMSO-d_6): δ (pmm) 167.90, 160.95, 154.166, 134.54, 129.48, 126.87, 125.34, 124.47, 122.73, 122.56, 116.54. ESI-MS $[M+H]^+$: calcd for $C_{13}H_9NOS$, 227.28; found 228.18.

*3.2.1.5. 2-(4-methoxyphenyl)-benzo[d]thiazole **(4e)***. Yield 82%; white solid; m.p. 118–119 °C; UV λmax 321.4 nm. IR (KBr) cm^{-1}: 2996.0, 2835.9, 1589.1, 1433.6, 1224.4, 1170.7, 751.7. ^{1}H NMR (400.0 MHz, DMSO-d_6): δ (ppm) 8.24 (d, J = 8.0 Hz, 1H, BTZ), 8.18 (d, J = 8.0 Hz, 1H, BTZ), 7.90 (d, J = 8.0 Hz, 2H, Ar), 7.75 (t, J = 6.4 Hz, 1H, BTZ), 7.70 (t, J = 6.4 Hz,1H, BTZ), 7.17 (d, J = 8.4 Hz, 2H, Ar), 3.92 (s, 3H, OCH_3). ^{13}C NMR (400 MHz, DMSO-d_6): δ (pmm) 167.50, 162.23, 154.09, 134.65, 129.33, 126.99, 125.95, 125.57, 122.90, 122.67, 115.21, 55.95. ESI-MS $[M+H]^+$: calcd for $C_{14}H_{11}NOS$, 241.06: found 242.27.

*3.2.1.6. 2-(2,4-dihydroxyphenyl)-benzo[d]thiazole **(4f)***. Yield 68%; yellow solid; m.p. 212–213 °C; UV λmax 337.0 nm. IR (KBr) cm^{-1}: 3446.7, 1599.8, 1474.3, 1217.2, 756.9. ^{1}H NMR (400 MHz, DMSO-d_6): δ (ppm) 9.22 (brs, 2H, OH), 8.18 (d, J = 8.0HZ, 1H, BTZ), 8.01 (d, J = 8.0HZ, 1H, BTZ), 7.56–7.46 (m, 3H, 2H BTZ, 1H Ar), 6.42 (d, J = 8 Hz, 1H, Ar), 6.33(s, 1H, Ar). ^{13}C NMR (400 MHz, DMSO-d_6): δ (pmm) 162.01, 158.65, 151.91, 133.73, 130.48, 126.78, 124.95, 122.31, 121.86, 110.65, 108.89, 103.072. ESI-MS $[M+H]^+$: calcd for $C_{13}H_9NO_2S$, 243.04; found 244.11.

*3.2.1.7. 2-(2,5-dihydroxyphenyl)-benzo[d]thiazole **(4g)***. Yield 58%; yellow solid; m.p. 220–221 °C; UV λmax 295.2, 362.8 nm. IR (KBr) cm^{-1}: 3332.8, 1579.8, 1496.0, 1197.2, 756.5. ^{1}H NMR (400.0 MHz, DMSO-d_6): δ(ppm) 10.82 (brs, 1H, OH), 9.18 (brs, 1H, OH), 8.17 (d, J = 8.0 Hz, 1H, BTZ), 8.01 (d, J = 8.0 Hz, 1H, BTZ), 7.59–7.38 (m, 2H BTZ, 1H Ar), 6.98–6.82 (m, 2H, Ar). ^{13}C NMR (400 MHz, DMSO-d_6): δ (pmm) 165.47, 151.93, 150.53, 149.68, 134.83, 126.85, 125.43, 122.51, 122.43, 120.73, 118.82, 118.31, 113.51. ESI-MS $[M+H]^+$: calcd for $C_{13}H_9NO_2S$, 243.04; found 244.14.

*3.2.1.8. 2-(3,4-dihydroxyphenyl)-benzo[d]thiazole **(4h)***. Yield 70%; yellow solid; m.p. 216–217 °C; UV λmax 329.2 nm. IR (KBr) cm^{-1}: 3488.6, 2916.8, 1599.1, 1474.3, 1260.5, 754.1. ^{1}H NMR (400 MHz, DMSO-d_6): δ (ppm) 9.51 (brs, 2H, OH), 8.12 (d, J = 8.0 Hz, 1H, BTZ), 7.98 (d, J = 8.0 Hz, 1H, BTZ), 7.51 (m, 2H, BTZ), 7.38 (m, 2H, Ar), 6.88 (d, J = 8.4 Hz, 1H, Ar). ^{13}C NMR (400 MHz, DMSO-d_6): δ (pmm) 168.10, 154.06, 149.40, 146.22, 134.47, 126.88, 125.34, 124.73, 122.52, 119.92, 118.56, 116.54, 114.36. ESI-MS $[M+H]^+$: calcd for $C_{13}H_9NO_2S$, 243.04; found 244.29.

*3.2.1.9. 2-(3-hydroxy-4-methoxyphenyl)-benzo[d]thiazole **(4i)***. Yield 65%; white solid; m.p. 184–185 °C; UV λmax 326.4 nm. IR (KBr) cm^{-1}: 3252.3, 1597.4, 1474.3, 1122.7, 763.9. ^{1}H NMR (400 MHz, DMSO-d_6): δ (ppm) 9.49 (brs, 1H, OH), 8.08 (d, J = 8.0 Hz, 1H, BTZ), 7.98 (d, J = 8.0 Hz, 1H, BTZ), 7.56–7.46 (m, 3H, 1H BTZ, 2H Ar), 7.40 (t, J = 7.2 Hz, 1H, BTZ), 7.01(d, J = 8.4 Hz, 1H, Ar), 3.85 (s, 3H, Ar). ^{13}C NMR (400 MHz, DMSO-d_6): δ (pmm) 167.77, 154.04, 151.07, 147.37, 134.62, 126.93, 126.07, 125.50, 122.85, 122.57, 119.62, 113.98, 112.76, 56.12. ESI-MS $[M+H]^+$: calcd for $C_{14}H_{11}NO_2S$, 257.31; found 258.29.

*3.2.1.10. 2-(3,5-dihydroxyphenyl)-benzo[d]thiazole **(4j)***. Yield 58%; yellow solid; m.p. 225–226 °C; UV λmax 302.0 nm. IR (KBr) cm^{-1}: 3068.7, 1606.9, 1438.3, 1147.9, 755.6. ^{1}H NMR (400 MHz, DMSO-d_6): δ (ppm) 10.01–10.22(brs, 2H, OH), 8.05 (d, J = 8.0 Hz, 1H, BTZ), 7.96 (d, J = 8.0 Hz, 1H, BTZ), 7.38–7.56 (m, 2H, BTZ), 6.96 (d, J = 2.0 Hz, 2H, Ar), 6.39 (s, 1H, Ar). ^{13}C NMR (400 MHz, DMSO-d_6): δ (pmm) 167.43, 158.96, 153.35, 134.28, 134.13, 126.45, 125.33, 122.70, 122.16, 105.34, 105.05. ESI-MS $[M+H]^+$: calcd for $C_{13}H_9NO_2S$, 243.04; found 244.19.

*3.2.1.11. 2-(2,4,5-trihydroxyphenyl)-benzo[d]thiazole **(4k)***. Yield 51%; grey solid; m.p. 225–226 °C; UV λmax 295.6, 365.4 nm. IR (KBr) cm^{-1}: 3068.8, 1603.2, 1437.8, 1150.3, 756.1. ^{1}H NMR (400 MHz, DMSO-d_6): δ (ppm) 9.48 (brs, 3H, OH), 8.16 (d, J = 8.0 Hz, 1H, BTZ), 8.01 (d, J = 8.0 Hz, 1H, BTZ), 7.64 (m, 2H, BTZ), 6.65 (s, 1H, Ar), 6.32 (s, 1H, Ar). ^{13}C NMR (400 MHz, DMSO-d_6): δ (pmm) 166.73, 151.51, 150.86, 150.39, 138.90, 133.29, 126.16, 124.21, 121.70, 121.19, 113.37, 108.68, 103.48. ESI-MS $[M+H]^+$: calcd for $C_{13}H_9NO_3S$, 259.03; found 260.18.

Following the general procedure compounds **6** and **7** were prepared and their analytical and spectra dare are in agreement with those reported in literature [44].

*3.2.2. 2-aminobenzo[d]thiazole-6-sulfonamide **(9)***

4-amino-benzenesulfonamide (5.00 g, 0.029 mol) and potassium thiocyanate (5.64 g, 0.058 mol) were dissolved in glacial acetic acid (45 mL). The mixture was stirred at room temperature for 20 min and then a bromine solution (1.49 mL 0.029 mol) in acetic acid glacial (5 mL) was added with a dropping funnel. After the addition, the mixture was kept under stirring at room temperature for 24 h. The precipitated solids were collected by filtration and obtained solid was dissolved in $H_2O{\cdot}NH_3$ 30% (about 2 mL) was added to the solution to bring the solution up to a pH8-9 and placed in the refrigerator overnight. The precipitated solids were collected by filtration and the product was washed with H_2O. The white product was dried and purified by recrystallization in EtOH to obtain 3.01 g of **9** as a white solid, with a yield of 45%. m.p. > 250 °C. UV λmax 305.90 nm. ^{1}H NMR (400 MHz,

DMSO-d_6): δ (ppm) δ 8.23 (1H, d), 7.96–7.84 (2H, dd), 7.02–6.83 (2H, d). ^{13}C NMR (400 MHz, DMSO-d_6): δ (pmm) 166.53, 156.34, 136.10, 125.36, 123.63, 121.59, 115.33. ESI-MS $[M+H]^+$: calcd for $C_7H_7N_3O_2S_2$, 229.28; found 230.09.

*3.2.3. bis(2-amino-4-benzenesulfonamide) disulfide (**10**)*

To the 2-amino-benzotiazole-6-sulfonamide (3 g, 0.013 mol), a KOH solution (3.95 g of KOH in 5.8 mL of H_2O) was added, which was subsequently refluxed for 8 h. After cooling, 35% HCl (about 2 mL) was added at −5° C until PH ≈ 8. The mixture was placed in refrigerator, left overnight and then filtered. The solid product was washed with H_2O and subsequently dried and recrystallized in EtOH to obtain 2.20 g (0.0054 mol) of **10** as a yellow solid, with a yield of 32%. m.p. 243–249 °C. UV λmax 355.1 nm. ^{1}H NMR (400 MHz, DMSO-d_6): δ (ppm 7.59 (1H, d, H_6), 7.39(1H, m), 7.28 (2H, brs), 6.75(1H, m), 6.26 (2H, br). ^{13}C NMR (400 MHz, DMSO-d_6): δ (pmm) 153.03, 133.99, 130.72, 129.60, 115.52, 114.59. ESI-MS $[M+H]^+$: calcd for $C_{12}H_{14}N_4O_4S_4$, 405.99; found 406.45.

3.2.4. General method for the synthesis of 2-Arylbenzothiazoles substituted on the benzothiazole ring

To a solution of 4-amino-3-mercaptobenzoic acid (0.49 g, 2.9 mmol) or bis(2-amino-4-benzenesulfonamide) disulfide (2.35 g, 5.8 mmol) and corresponding benzaldehydes in ethanol (10 mL) was added a solution of sodium hydrosulfite (1 eq. in 5 mL H_2O) at room temperature. The mixture was heated at reflux for 36 h. After cooling, the solution was concentrated in vacuum. The residue was treated with HCl 2 N (15 mL) and filtered to obtain the crude solid, which was recrystallized in MeOH/H_2O.

*3.2.4.1. 2-(2-hydroxyphenyl)benzo[d]thiazole-6-carboxylic acid (**11b**)*. Yield 71%; yellow solid; m.p. > 250 °C; UV λmax 338.5 nm. IR (KBr) cm^{-1}: 3111.6, 1677.8, 1590.6, 1481.8, 1217.7, 1167.1, 739.9. ^{1}H NMR (400 MHz, DMSO-d_6) δ (pmm) 11.40 (br, 1H, COOH), 9.82 (brs, 1H, OH), 8.61 (s, 1H, BTZ), 8.12 (d, J = 8.4 Hz, 1H, BTZ), 7.74.7.68 (m, 2H, 1H BTZ, 1H Ar), 7.47 (t, J = 6.8 Hz, 1H, Ar), 7.21–7.16 (m, 2H, Ar). ^{13}C NMR (400 MHz, DMSO-d_6): δ(ppm) 173.46, 171.10, 153.55, 143.3, 132.48, 131.85, 129.48, 127.48, 127.33, 124.28, 122.50, 119.53, 118.78, 115.88. ESI-MS $[M+H]^+$: calcd for $C_{14}H_9NO_3S$, 271.03; found 272.24.

*3.2.4.2. 2-(3-hydroxyphenyl)benzo[d]thiazole-6-carboxylic acid (**11c**)*. Yield 55%; yellow solid; m.p. > 250 °C; UV λmax 301.1 nm. IR (KBr) cm^{-1}: 3110.6, 1676.6, 1582.6, 1481.6, 1217.6, 1142.4, 769.5. ^{1}H NMR (400 MHz, DMSO-d_6): δ (ppm) 11.62 (brs, 1H, -COOH), 9.34 (brs, 1H, OH), 8.49 (s, 1H, BTZ), 8.02 (d, J = 8.4 Hz, 1H, BTZ), 7.71 (d, J = 8.4 Hz, 1H, BTZ), 7.56 (d, J = 8.4 Hz, 1H, Ar), 7.28 (t, 1H, Ar), 7.11 (s, 1H, Ar), 6.95 (d, J = 8.4 Hz, 1H, Ar). ^{13}C NMR (400 MHz, DMSO-d_6): δ(ppm) 167.38, 167.20, 156.84, 153.86, 146.96, 134.64, 132.67, 128.38, 127.21, 123.68, 121.49, 119.30, 118.58, 116.96. ESI-MS $[M+H]^+$: calcd for $C_{14}H_9NO_3S$, 271.03; found 272.31.

*3.2.4.3. 2-(4-hydroxyphenyl)benzo[d]thiazole-6-carboxylic acid (**11d**)*. Yield 67%; yellow solid; m.p. > 250 °C; UV λmax 334.3 nm. IR (KBr) cm^{-1}: 3259.1, 1680.9, 1587.4, 1418.4, 1240.2, 1167.0, 770.5. ^{1}H NMR (400 MHz, DMSO-d_6): δ (ppm) 10.89 (brs, 1H, OH), 9.78 (brs, 1H, OH), 8.68 (s, 1H, BTZ), 8.05 (d, J = 8.4 Hz, 1H, BTZ), 7.72 (d, J = 8.4 Hz, 1H, BTZ), 7.59 (d, J = 8.4 Hz, 2H Ar), 6.99 (d, J = 8.4 Hz, 2H, Ar). ^{13}C NMR (400 MHz, DMSO-d_6): δ(ppm) 177.53, 167.38, 161.56, 157.00, 134.70, 132.53, 131.18, 129.82, 127.88, 127.43, 124.59, 124.12, 122.41, 116.65. ESI-MS $[M+H]^+$: calcd for $C_{14}H_9NO_3S$, 271.03; found 272.20.

*3.2.4.4. 2-(4-methoxyphenyl)benzo[d]thiazole-6-carboxylic acid (**11e**)*. Yield 82%; yellow solid; m.p. > 250 °C; UV λmax 331.9 nm. IR (KBr) cm^{-1}: 2980.8, 1683.0, 1592.8, 1480.2, 1263.2, 1085.4, 712.0. ^{1}H NMR (400 MHz, DMSO-d_6): δ (ppm) 9.87 (brs, 1H, OH), 8.75 (s, 1H, BTZ), 8.17 (d, J = 8.4 Hz, 1H, BTZ), 7.87 (d, J = 8.4 Hz, 1H, BTZ), 7.14 (m, 4H, Ar) 3.8 (s, 3H, OCH_3). ^{13}C NMR (400 MHz, DMSO-d_6): δ(ppm) 179.26, 170.57, 166.81, 162.12, 156.44, 134.28, 129.11, 127.38, 125.11, 124.14, 122.06, 114.77, 65.42. ESI-MS $[M+H]^+$: calcd for $C_{15}H_{11}NO_3S$, 285.32; found 286.27.

*3.2.4.5. 2-(2,4-dihydroxyphenyl)benzo[d]thiazole-6-carboxylic acid (**11f**)*. Yield 53%; yellow solid; m.p. > 250 °C; UV λmax 345.5 nm. IR (KBr) cm^{-1}: 3351.2, 1674.1, 1577.9, 1481.5, 1216.8, 1090.2, 779.9. ^{1}H NMR (400 MHz, DMSO-d_6): δ (ppm) 10.22 (brs, 2H, OH), 8.79 (s, 1H, BTZ), 7.99 (dd, J = 8 hz, J = 1.6 Hz, 2H, BTZ), 7.79 (d, J = 8.4 Hz, 1H, Ar), 6.58 (s, 1H, Ar), 6.39 (d, J = 8.4 Hz, 1H, Ar). ^{13}C NMR (400 MHz, DMSO-d_6): δ (ppm) 169.42, 166.99, 162.11, 152.93, 135.48, 133.66, 129.89, 128.16, 122.84, 120.21, 111.51, 108.04, 104.64, 103.29. ESI-MS $[M+H]^+$: calcd for $C_{14}H_9NO_4S$, 287.29; found 288.30.

*3.2.4.6. 2-(2,5-dihydroxyphenyl)benzo[d]thiazole-6-carboxylic acid (**11g**)*. Yield 75%; yellow solid; m.p. > 250 °C; UV λmax 305.9, 371.6 nm. IR (KBr) cm^{-1}: 3440.7, 2533.3, 1676.8, 1596.9, 1493.6, 1288.5, 1180.4, 780.5. ^{1}H NMR (400 MHz, DMSO-d_6): δ (ppm) 13.07 (brs, 1H, OH), 10.82 (s, 1H, OH), 9.19 (s, 1H, OH), 8.71 (d, J = 1.2 Hz, 1H, BTZ), 8.07–8.02 (m, 2H, BTZ), 7.67(d, J = 2.8 Hz, 1H, Ar), 6.85–6.92 (m, 2H, Ar). ^{13}C NMR (400 MHz, DMSO-d_6): δ (ppm), 167.50, 154.77, 149.91, 127.64, 124.52, 122.25, 121.25, 119.14, 118.28, 113.48, 110.00. ESI-MS $[M+H]^+$: calcd for $C_{14}H_9NO_4S$, 287.29; found 288.23.

*3.2.4.7. 2-(3,4-dihydroxyphenyl)benzo[d]thiazole-6-carboxylic acid (**11h**)*. Yield 69%; yellow solid; m.p. > 250 °C; UV λmax 346.2 nm. IR (KBr) cm^{-1}: 3487.4, 1681.8, 1594.1, 1417.7, 1274.7, 1180.8, 770.3. ^{1}H NMR (400 MHz, DMSO-d_6): δ (ppm) 12.90 (brs, 1H, OH), 9.78 (s, 1H, OH), 9.45 (s, 1H, OH), 8.64 (s, 1H, BTZ), 8.02 (m, 2H, 1H BTZ, 1H Ar), 7.55 (d, J = 1.2 Hz, 1H, BTZ), 7.43 (d, J = 8.2 Hz, 1H, Ar), 6.92 (d, J = 8.2 Hz, 1H, Ar). ^{13}C NMR (400 MHz, DMSO-d_6): δ (ppm) 171.12, 166.85, 156.46, 149.48, 145.77, 134.12, 127.29, 126.81, 123.99, 123.89, 121.83, 119.77, 116.09, 114.00. ESI-MS $[M+H]^+$: calcd for $C_{14}H_9NO_4S$, 287.23; found 288.23.

*3.2.4.8. 2-(3-hydroxy-4-methoxyphenyl)benzo[d]thiazole-6-carboxylic acid (**11i**)*. Yield 69%; yellow solid; m.p. > 250 °C; UV λmax 341.1 nm. IR (KBr) cm^{-1}: 3547.6, 2956.4, 1702.9, 1587.4, 1477.6, 1217.2, 1142.4, 769.5. ^{1}H NMR (400 MHz, DMSO-d_6): δ (ppm) 9.68 (brs, 1H, OH), 8.72 (s, 1H, BTZ), 8.05 (d, J = 8 Hz, 2H, BTZ), 7.58 (d, J = 8 Hz, 1H, Ar), 7.50 (s, 1H, Ar) 7.11 (d, J = 8 Hz, 1H, Ar), 3.84 (s, 3H, OCH_3). ^{13}C NMR (400 MHz, DMSO-d_6): δ (ppm) 171.11, 167.46, 156.74, 151.51, 147.47, 134.72, 127.93, 125.79, 124.52, 122.47, 119.93, 114.09, 112.82, 56.46. ESI-MS $[M+H]^+$: calcd for $C_{15}H_{11}NO_4S$, 301.04; found 302.19.

*3.2.4.9. 2-(3,5-dihydroxyphenyl)benzo[d]thiazole-6-carboxylic acid (**11j**)*. Yield 59%; yellow solid; m.p. > 250 °C; UV λmax 313.2 nm. IR (KBr) cm^{-1}: 3481.4, 1681.0, 1589. 8, 1423.2, 1270.1, 1182.9, 772.8. ^{1}H NMR (400 MHz, DMSO-d_6) δ: (ppm) 10.78 (brs, 2H, OH), 8.84 (s, 1H, BTZ), 8.18 (d, J = 8 Hz, 1H, BTZ), 7.85 (d, J = 8 Hz, 1H, BTZ), 6.95 (s, 2H, Ar), 6.25 (s, 1H, Ar). ^{13}C NMR (400 MHz, DMSO-d_6): δ (ppm) 170.10, 166.46, 158.73, 157.49, 136.60, 133.72, 133.63, 127.03, 123.92, 122.13, 105.51, 104.57. ESI-MS $[M+H]^+$: calcd for $C_{14}H_9NO_4S$, 287.23; found 288.12.

*3.2.4.10. 2-(2,4,5-trihydroxyphenyl)benzo[d]thiazole-6-carboxylic acid (**11k**)*. Yield 63%; grey solid; m.p. > 250 °C; UV λmax 378.0 nm. IR (KBr) cm^{-1}: 3498.0, 1689. 7, 1611.5, 1455.0, 1277. 5, 1186.0, 775.3. ^{1}H NMR (400 MHz, DMSO-d_6): δ (ppm) 10.24 (brs, 3H, OH), 8.90 (s, 1H, BTZ), 8.23(d, J = 8 Hz, 1H, BTZ), 8.07 (d, J = 8 Hz, 1H, BTZ), 6.96 (s, 1H, Ar), 6.19 (s, 1H, Ar). ^{13}C NMR (400 MHz, DMSO-d_6): δ (ppm) 170.45, 166.11, 157.14, 155.56, 149.12, 138.45, 135.38, 126.70, 125.76, 122.09, 121.05, 113.41, 108.50, 107.17. ESI-MS [M

+H]$^+$: calcd for $C_{14}H_9NO_5S$, 303.02; found 304.23.

3.2.4.11. 2-(2-hydroxyphenyl)benzo[d]thiazole-6-sulfonamide ***(11m)***. Yield 78%; yellow solid; m.p. > 250 °C; UV λmax 335.6 nm. IR (KBr) cm^{-1}: 3316.0, 3242.7, 1584.2, 1483.7, 1312.7, 1151.5, 746.0. ^{1}H NMR (400 MHz, DMSO-d_6): δ 9.82 (brs, 1H, OH), 8.48 (s, 1H, BTZ), 7.96 (d, J = 8.2 Hz, 1H, BTZ), 7.82 (d, J = 8.2 Hz, 1H, BTZ), 7.64 (d, J = 8.2 Hz, 1H, Ar), 7.36 (t, 1H, Ar), 7.28 (brs, 2H, NH_2), 7.08–6.95(m, 2H, Ar). ^{13}C NMR (400 MHz, DMSO-d_6): δ (ppm) 177.67, 156.83, 154.66, 140.63, 135.33, 133.45, 129.02, 124.35, 122.86, 120.47, 120.04, 119.09, 117.34. ESI-MS [M+H]$^+$: calcd for $C_{13}H_{10}N_2O_3S_2$, 306.01; found 307.19.

3.2.4.12. 2-(3-hydroxyphenyl)benzo[d]thiazole-6-sulfonamide ***(11n)***. Yield 78%; yellow solid; m.p. > 250 °C; UV λmax 299.5 nm. IR (KBr) cm^{-1}: 3312.9, 3206.3, 1584.6, 1461.6, 1300.8, 1290.4, 1152.4, 780.0. ^{1}H NMR (400 MHz, DMSO-d_6): δ (ppm) 9.28 (brs, 1H, OH), 8.51 (s, 1H, BTZ), 8.02 (d, J = 8.2 Hz, 1H, BTZ), 7.88 (d, J = 8.2 Hz, 1H, BTZ), 7.54 (d, J = 8.2 Hz, 1H, Ar), 7.38-0.26 (m, 2H, Ar), 7.18 (brs, 2H, NH_2), 6.83 (d, J = 8.2 Hz, 1H, Ar). ^{13}C NMR (400 MHz, DMSO-d_6): δ (ppm) 170.95, 157.96, 155.05, 140.75, 134.35, 133.47, 130.59, 124.08, 123.05, 120.55, 119.05, 118.23, 113.45. ESI-MS [M+H]$^+$: calcd for $C_{13}H_{10}N_2O_3S_2$, 306.01; found 307.22.

3.2.4.13. 2-(4-hydroxyphenyl)benzo[d]thiazole-6-sulfonamide ***(11o)***. Yield 84%; yellow solid; m.p. > 250 °C; UV λmax 331.2 nm. IR (KBr) cm^{-1}: 3337.2, 3230.2, 1605.7, 1478.3, 1303.0, 1273.0, 1147.8, 832.8. ^{1}H NMR (400 MHz, DMSO-d_6): δ (ppm) 10.39 (brs, 1H, OH), 8.58 (s, 1H, BTZ), 8.15 (d, J = 8.2 Hz, 1H, BTZ), 7.94 (d, J = 8.2 Hz, 1H, BTZ), 7.84 (dd, J = 8.2 Hz, J = 1.6 Hz, 2H, Ar), 7.44 (brs, 2H, NH_2), 6.96 (d, J = 8.2 Hz, 2H, Ar). ^{13}C NMR (400 MHz, DMSO-d_6): δ (ppm) 169.19, 157.72, 152.48, 136.42, 133.16, 129.03, 127.29, 125.95, 123.95, 122.28, 116.56. ESI-MS [M+H]$^+$: calcd for $C_{13}H_{10}N_2O_3S_2$, 306.01; found 307.12.

3.2.4.14. 2-(4-methoxyphenyl)benzo[d]thiazole-6-sulfonamide ***(11p)***. Yield 80%; yellow solid; m.p. > 250 °C; UV λmax 328.3 nm. IR (KBr) cm^{-1}: 3329.4, 3258.2, 1605.4, 1480.2, 1304.0, 1261.2, 1165.2, 829. 9. ^{1}H NMR (400 MHz, DMSO-d_6): δ (ppm) 8.59 (s, 1H, BTZ), 8.17 (d, J = 8.2 Hz, 1H, BTZ), 8.09 (dd, J = 8.2 Hz, J = 1.6 Hz, 2H, Ar), 7.97 (d, J = 8.2 Hz, 1H, BTZ), 7.43 (brs, 2H, NH_2), 7.18 (d, J = 8.2 Hz, 2H, Ar), 3.83 (s, 3H, -OCH_3). ^{13}C NMR (400 MHz, DMSO-d_6): δ (ppm) 171.19, 162.72, 155.81, 140.90, 134.75, 129.70, 125.50, 124.60, 123.14, 120.96, 115.34, 56.02. ESI-MS [M+H]$^+$: calcd for $C_{14}H_{12}N_2O_3S_2$, 320.03; found 321.23.

3.2.4.15. 2-(2,4-dihydroxyphenyl)benzo[d]thiazole-6-sulfonamide ***(11q)***. Yield 74%; yellow solid; m.p. > 250 °C; UV λmax 344.5 nm. IR (KBr) cm^{-1}: 3338.4, 3230.1, 1592.6, 1474.6, 1340.1, 1296.7, 1150.5, 807.5. ^{1}H NMR (400 MHz, DMSO-d_6): δ (ppm) 9.84 (brs, 1H, OH), 9.76 (brs, 1H, OH), 8.50 (s, 1H, BTZ), 8.02 (d, J = 8.2 Hz, 1H, BTZ), 7.88 (d, J = 8.2 Hz, 1H, BTZ), 7.52 (d, J = 8.2 Hz, 1H, Ar), 7.21 (brs, 2H, NH_2), 6.48 (m, 1H, Ar), 6.31 (s, 1H, Ar) . ^{13}C NMR (400 MHz, DMSO-d_6): δ (ppm) 168.84, 162.47, 153.86, 139.97, 133.98, 130.61, 129.60, 124.24, 122.02, 120.46, 114.59, 109.05, 102.97. ESI-MS [M+H]$^+$: calcd for $C_{13}H_{10}N_2O_4S_2$, 322.01; found 323.14.

3.2.4.16. 2-(2,5-dihydroxyphenyl)benzo[d]thiazole-6-sulfonamide ***(11r)***. Yield 55%; yellow solid; m.p. > 250 °C; UV λmax 301.0, 369.0 nm. IR (KBr) cm^{-1}: 3347.9, 3263.1, 1601.6, 1496.5, 1342.4, 1215. 5, 1155.5, 765.5. ^{1}H NMR (400 MHz, DMSO-d_6): δ (ppm) 10.82 (brs, 1H, OH), 9.2 (brs, 1H, OH), 8.60 (s, 1H, BTZ), 8.19 (d, J = 8.2 Hz, 1H, BTZ) , 7.98 (dd, J = 8.2 Hz, J = 1.6 Hz, 1H, BTZ), 7.64 (d, J = 1.6 Hz, 1H, Ar), 7.42 (brs, 2H, NH_2), 6.98–6.83 (m, 2H, Ar). ^{13}C NMR (400 MHz, DMSO-d_6): δ (ppm) 167.95, 153.67, 150.57, 149.88, 140.51, 135.44, 124.29, 122.78, 121.32, 120.68, 119.14, 118.27, 113.46. ESI-MS [M+H]$^+$: calcd for $C_{13}H_{10}N_2O_4S_2$, 322.01; found 322.19.

3.2.4.17. 2-(3,4-dihydroxyphenyl)benzo[d]thiazole-6-sulfonamide ***(11s)***. Yield 69%; yellow solid; m.p. > 250 °C; UV λmax 344.1 nm. IR (KBr) cm^{-1}: 3499.0, 3307.1, 1603.0, 1490.8, 1335.7, 1279.3, 1145.2, 825.2. ^{1}H NMR (400 MHz, DMSO-d_6): δ (ppm) 9.37 (brs, 2H, OH), 8.47 (s, 1H, BTZ), 8.12 (d, J = 8.2 Hz, 1H, BTZ), 7.94 (d, J = 8.2 Hz, 1H, BTZ), 7.41 (brs, 2H, NH_2), 7.28 (d, J = 8.2 Hz, 1H, Ar), 7.03 (s, 1H, Ar), 6.81 (d, J = 8.2 Hz, 1H, Ar). ^{13}C NMR (400 MHz, DMSO-d_6): δ (ppm) 170.12, 155.36, 149.55, 145.80, 140.09, 134.04, 123.92, 123.74, 122.30, 120.25, 119.77, 116.12, 114.04. ESI-MS [M+H]$^+$: calcd for $C_{13}H_{10}N_2O_4S_2$, 322.01; found 322.16.

3.2.4.18. 2-(3-hydroxy-4-methoxyphenyl)benzo[d]thiazole-6-sulfonamide ***(11t)***. Yield 78%; yellow solid; m.p. > 250 °C; UV λmax 354.8 nm. IR (KBr) cm^{-1}: 3329.4, 2957.7, 1605.4, 1486.5, 1313.4, 1270.8, 1169. 9, 826.4. ^{1}H NMR (400 MHz, DMSO-d_6): δ (ppm) 9.41 (brs, 1H, OH), 8.48 (s, 1H, BTZ), 8.06 (d, J = 8.1 Hz, 1H, BTZ), 7.92 (d, J = 8.1 Hz, 1H, BTZ), 7.47 (d, J = 8.1 Hz, 1H, Ar), 7.33 (brs, 2H, NH_2), 7.16 (s, 1H, Ar), 6.94 (d, J = 8.1 Hz, 1H, Ar), 3.88 (s, 3H, -OCH_3). ^{13}C NMR (400 MHz, DMSO-d_6): δ (ppm) 168.05, 155.54, 148.98, 145.92, 142.11, 134.51, 122.43, 122.01, 121.79, 120.00, 118.70, 116.86, 114.04, 56.98. ESI-MS [M+H]$^+$: calcd for $C_{14}H_{12}N_2O_4S_2$, 336.02; found 337.38.

3.2.4.19. 2-(3,5-dihydroxyphenyl)benzo[d]thiazole-6-sulfonamide ***(11u)***. Yield 63%; yellow solid; m.p. > 250 °C; UV λmax 354.1 nm. IR (KBr) cm^{-1}: 3499. 7, 3312.1, 1623.3, 1492.2, 1338.2, 1278. 9, 1144.6, 826.1. ^{1}H NMR (400 MHz, DMSO-d_6): δ (ppm) 9.48 (brs, 2H, OH), 8.39 (s, 1H, BTZ), 8.01 (d, J = 8.1 Hz, 1H, BTZ), 7.86 (d, J = 8.1 Hz, 1H, BTZ), 7.40 (brs, 2H, NH_2), 6.91 (s, 2H, Ar), 6.35 (s, 1H, Ar). ^{13}C NMR (400 MHz, DMSO-d_6): δ (ppm) 166.43, 158.23, 157.17, 137.56, 132.80, 132.02, 127.43, 123.55, 122.37, 105.98, 104.24. ESI-MS [M+H]$^+$: calcd for $C_{13}H_{10}N_2O_4S_2$, 322.01; found 323.04.

3.2.4.20. 2-(2,4,5-trihydroxyphenyl)benzo[d]thiazole-6-sulfonamide ***(11v)***. Yield 51%; grey solid; m.p. > 250 °C; UV λmax 353.9 nm. IR (KBr) cm^{-1}: 3350.3, 3264. 8, 1609.5, 1495. 8, 1341.9, 1216.3, 1157.4, 766.8. ^{1}H NMR (400 MHz, DMSO-d_6): δ (ppm) 9.57 (brs, 3H, OH), 8.39 (s, 1H, BTZ), 8.08 (d, J = 8.2 Hz, 1H, BTZ), 7.91 (d, J = 8.2 Hz, 1H, BTZ), 7.32 (brs, 2H, NH_2), 6.88(s, 1H, Ar), 6.41 (s, 1H, Ar). ^{13}C NMR (400 MHz, DMSO-d_6): δ (ppm) 166.61, 157.90, 150.80, 149.87, 138.15, 133.86, 126.90, 124.45, 121.84, 121.60, 113.90, 111.24, 105.56. ESI-MS [M+H]$^+$: calcd for $C_{13}H_{10}N_2O_5S_2$, 338.00; found 339.18.

3.3. Biological studies

3.3.1. Antioxidant activity assays

Free radical Scavenging Activity on DPPH. The following assay is modified procedure described by Wang at al. [63] The methanolic solution of DPPH (1.5 mL) was added to 0.750 mL of tested sample solutions (solubilized in DMSO and diluted in MeOH) at different concentrations (1, 0.5, 0.25, 0.125 and 0.0625 mg/mL). The samples were kept in the dark at room temperature. After 30 min, the absorbance values were measured using UV–VIS spectrophotometer at 517 nm using UV–VIS spectrophotometer and were converted into the percentage antioxidant activity (%) using the Eq. (1).

$$\mathrm{DPPH\backslash;radical-scavenging\backslash;capacity\backslash;(\%)} = [1 - A_1/A_0] \times 100\% \quad (1)$$

where A_0 was the absorbance of the control (without sample) and A_1 was the absorbance in the presence of the sample. Linear regression a plot is carried out for calculating the effective concentration of the sample required to scavenge 50% of DPPH free radicals.

Ferric Reducing Antioxidant Power (FRAP) assay. Ferric reducing antioxidant power (FRAP) assay is a widely used method that uses antioxidants as reductants in a redox-linked colorimetric reaction and it

is based on the reduction of ferric ions (Fe^{3+}) to ferrous ions (Fe^{2+}) in the presence of TPTZ (2,4,6- tripyridyl-striazine). This reaction is monitored by measuring the change in absorbance at 593 nm. The analysis reagent was prepared according to Benzie [64] procedure by mixing the following solutions in the reported ratio 10/1/1 (v:v:v): i) 0.1 M acetate buffer pH 3.6, ii) TPTZ 10 mmol/L in 40 mmol/ HCl, iii) ferric chloride 20 mmol/L. To 1.9 mL of reagent were added 0.1 mL of sample proper diluted or solvent when blank was performed. FRAP values are obtained by comparing the absorbance change at 593 nm in sample solution with the absorbance of the blank reaction, using a UV–VIS spectrophotometer.

3.3.2. In vitro Photoprotection assay

3.3.2.1. Evaluation of filtering parameters of compounds in solution. Sun protection factor evaluation was performed by means of a UV–VIS spectrophotometer SHIMADZU UV-2600 240 V. Test compounds were dissolved in dimethylsulfoxide at the concentration of 0.0015 (± 0.000005) % and the absorbance was measured between 290 and 400 nm using a 1 cm quartz cell at intervals of one 1 nm using a UV–Vis Spectrophotometer. The absorbance at wavelength λ is related to the transmittance (T(λ)) by the Eq. (2)

$$A(\lambda) = -\mathrm{Log}[T(\lambda)] \tag{2}$$

where T(λ) is the fraction of incident irradiance transmitted by the sample.

3.3.2.2. In vitro evaluation of filtering parameters of formulation. The selected synthesized molecules were included at the concentration of 1% in a topical formulation O/W in order to evaluate their UV -filter activity

INCI: aqua, glycerin, Euxyl PE 9010, Xanthan gum, ceteareth-12, ceteareth-20, Sterearic acid, Butylhydroxytoluene, Myritol, PEG-7 glycerylcocoate and sodium solution 10%.

WW5 PMMA plates have been purchased from Schonberg GmbH (Munich, Germany). 32.5 mg of each compound formulation O/W were spread onto 5 × 5 cm^2 PMMA plates in small droplets of approximately equal mass evenly distributed over the rough surface of the plate. For each product, three plates were prepared and left to dry at room temperature in the dark for 15–30 min before exposure, in order to facilitate the formation of a standard stabilized sunscreen film. After this period, the plates were placed in the light path of the transmittance analyzer. Then the measure of UV transmittance was carried out from 290 to 400 nm on 5 different sites of each plate. The blank was prepared using a plate covered with 32.5 mg of glycerin. This substrate allows to have a reference spectrum with a transmission close to 100% due to its non-fluorescent and UV transparency.

Moreover, Values of *in vitro* SPF, UVA-PF and Critical Wavelength were calculated according to Eq. (3), Eq. (4) and Eq. (5) [65] respectively using SPF Calculator Software (SPF Calculator Software (version 2.1), Shimadzu, Milan, Italy).

$$\mathrm{SPF_{invitro}} = \frac{\int_{\lambda=290\mathrm{nm}}^{\lambda=400\mathrm{nm}} E(\lambda)\times I(\lambda)\times d\lambda}{\int_{\lambda=290\mathrm{nm}}^{\lambda=400\mathrm{nm}} E(\lambda)\times I(\lambda)\times 10^{-A_0(\lambda)}\times d\lambda} \tag{3}$$

where E(λ) is the erythema action spectrum, I (λ) is the spectral irradiance of the UV source, $A_0(\lambda)$ is the monochromatic absorbance of the test sample before UV exposure, and dλ is the wavelength step (1 nm)

$$\mathrm{UVAPF} = \frac{\int_{\lambda=290\mathrm{nm}}^{\lambda=400\mathrm{nm}} P(\lambda)\times I(\lambda)\times d\lambda}{\int_{\lambda=290\mathrm{nm}}^{\lambda=400\mathrm{nm}} P(\lambda)\times I(\lambda)\times 10^{-A(\lambda)\times C}\times d\lambda} \tag{4}$$

where P(λ) is the persistent pigment darkening (PPD) action spectrum. C is the coefficient of adjustment. A(λ) is the mean monochromatic absorbance of the test product layer after UV exposure.

The wavelength at which the summed absorbance reaches 90% of total absorbance is defined as the critical wavelength. Therefore (T_λ) were converted into absorbance values A(λ) following Eq. (5) and final Critical Wavelength is:

$$\int_{290\mathrm{nm}}^{\lambda_c} A\lambda \times d\lambda = 0.9 \int_{290\mathrm{nm}}^{400\mathrm{nm}} A\lambda \times d\lambda \tag{5}$$

where A(λ): monochromatic absorbance calculated from transmittance at wavelength λ

3.3.3. Antifungal activity

3.3.3.1. Antidermatophyte activity. Microorganisms. The dermatophytes used were *Epidermophyton floccosum* var. floccosum (Netherlands) CBS 358.93 strain; *Trichophyton tonsurans* (Netherlands) CBS 483.76 strain; *Trichophyton mentagrophytes* (Netherlands) CBS 160.66 strain; *Microsporum canis* (Iran) CBS 131110 strain; and *Microsporum gypseum* (Iran) CBS 130948 strain. All dermatophytes were maintained at 4 °C as agar slants on Sabouraud dextrose agar (SDA; Sigma-Aldrich SRL, Milano, Italy).

Culture. In vitro antifungal activity against five dermatophytes was evaluated using plate growth rate method. Each compound was dissolved in DMSO. Suitable solution adjusted to 0.1% was added to the sterile culture medium (SDA) at 45 °C. The final concentration of the medium was 100 $\mu g{\cdot}mL^{-1}$. The mixture was homogenized and transferred to a sterile Petri dish to solidify. Inoculums were previously obtained by transplanting mycelium disks cut from the periphery of a single mother cultures, incubated on thin sheets of cellophane delicately extended on the agar plates and placed at 26 °C until the appearance of some characters that show how the fungus grew. According to the poisoned-food technique [66], inoculums were then transferred to analyzed Petri dish and incubated under growth conditions. The mixed medium (SDA + DMSO) without sample was used as the blank control. Antifungal activity was determined by measuring the diameter of the inhibition zone for seven days. Percentages of growth inhibition were calculated by comparing mean value of diameters of the mycelia in test plates with that of untreated control plates following the Eq. (6). The percent inhibition of growth was determined as the average of three different experiments.

$$I = [(C - T)/C]\cdot 100\%. \tag{6}$$

where I is the growth inhibition rate (%), C is the extended diameter of the circle mycelium of the control (mm), and T is the extended diameter of the circle during testing (mm).

3.3.3.2. Anti-Candida albicans activity. Stock solutions were prepared by dissolving the compounds and Fluconazole in DMSO at a concentration of 12.80 mg/mL. Minimal inhibitory concentration (MIC) of the synthesized agents was performed by broth microdilution method according to the Clinical and Laboratory Standards Institute/National Committee for Clinical Laboratory Standards (CLSI/NCCLS) Approved Standard M27-A3, 2008 [NCCLS]. RPMI 1640 was buffered with 0.165 M MOPS, solution was agitated and brought to pH 6.9 with a 1 N NaOH solution. The solution was filtered with 0.45 μm sterilized filter and stocked in fridge. Just before setting up the assay, further dilute of stock solutions was dilute in 1:10 RPMI supplemented with Tween 80 (used as blank). Dilutions, 11 increasing concentrations, ranging from 0.25 to 128 $\mu g{\cdot}mL^{-1}$ of the compounds, were prepared in 96-well plates. The inoculum size was about 2.5 × 10^3 $cells{\cdot}mL^{-1}$. The plates were incubated at 30 °C for 24–48 h.

3.3.4. Antiproliferative activity

Cell lines. Human cervical carcinoma (HeLa), human $CD_4{}^+$ *T*-lymphoblast (CEM) and human melanoma cells (SK-Mel 5) cells were obtained from ATCC (Middlesex, UK). Human pancreatic carcinoma (Mia-Paca 2) cells were kindly provided by Prof. Anna Karlsson (Karolinska

Institute, Stockholm, Sweden). All cell lines were grown in Dulbecco's modified Eagle's medium (DMEM; Gibco, Carlsbad, CA, USA), supplemented with 10% fetal bovine serum (FBS, Gibso), 0.01 M Hepes (Gibco) and 1 mM sodium pyruvate (Gibco) in a humidified 5% CO_2 incubator at 37 °C.

Cell proliferation. Suspension of CEM cells were seeded in 96-well microtiter plates at 60,000 cells/well in the presence of different concentrations of the compounds. The cells were allowed to proliferate for 48 h or 72 h, respectively, and then counted in a Coulter counter. The 50% inhibitory concentration (IC_{50}) was defined as the compound concentration required to reduce cell proliferation by 50%. HeLa and Mia-Paca2 cells were seeded in 96-well plates at 15,000 cells/well in the presence of different concentrations of the compounds. After 4 days of incubation, the cells were trypsinized and counted in a Coulter counter).

IC_{50} Determination. The compounds were dissolved in DMSO at 20 mM (stock solution) and kept in the refrigerator until use. Then, compound dilutions were made in cell culture medium, and serial compound concentrations were tested starting at 100 μM as the highest concentration. The DMSO concentration, present at the highest compound concentration was 0.5% that is at a concentration that did not affect the tumour cell proliferation. The IC_{50} values were calculated using Eq. (7).

$$C1 - [50 - N1\%/N2\% - N1\%] - (C1 - C2) \quad (7)$$

wherein C1 is the compound concentration that inhibits cell proliferation more than 50%; *C*2 is the compound concentration that inhibits cell proliferation less than 50%; N1% represents the cell number (in percent of control in the absence of compound) obtained in the presence of C1 and N2% represents the cell number (in percent of control in the absence of compound) obtained in the presence of *C*2.

3.3.5. HERG expressed in HEK

Cell line. Electrophysiology study was performed using HEK293 cells stably transfected with hERG cDNA.

Reagents and solutions. Test substances were formulated in 0.1% DMSO. Stock solutions were diluted in extracellular solution plus 0.05% Pluronic F-68 (Sigma), to final perfusion concentrations, which were 0.1, 1 and 10 μM. In positive control group, 0.003–0.03–0.3 μM E-4031 (Tocris) was assessed as a test compound. The mM composition of the extracellular solution was: NaCl, KCl, $CaCl_2$, $MgCl_2$, D-glucose, N-(2-hydroxyethyl)piperazine-N'-2-(ethanesulfonic acid) (HEPES), pH 7.4 with 1 M NaOH (137:4:1.8:1:10:10 respectively). The intracellular solution composition was (in mM): KCl, $MgCl_2$, Ethylene glycol-bis(ß-aminoethyl ether)-N,N,N',N'-tetraacetic acid (EGTA), MgATP, HEPES, pH 7.2 with 1 M KOH (130:1:5:5:10 respectively). The intracellular solution was filtered through a 0.2 μm polycarbonate membrane filter upon formulation. All reagents were purchased from Sigma-Aldrich.

Voltage protocol. The voltage protocol used to evaluate the effect of test substances on hERG channel current was as follows: step from −80 mV to –50 mV for 200 ms, +20 mV for 4.8 s, step to −50 mV for 5 s then step to the holding potential of −80 mV. The step from −80 mV to the test command (+20 mV) results in an outward current (i.e. current flows out of the cell) and the step from the test command (+20 mV) to −50 mV results in the tail current. The pulse pattern was repeated continuously at 15 *sec* intervals from a holding potential of −80 mV.

The voltage protocol was run and recorded continuously during the experiment. The stability of recording was assessed through initial wash with extracellular solution alone. The vehicle was then applied for 3 min followed by the test substance. The test substance was applied in triplicate to ensure adequate mixing. The standard combined exposure time was 5 min. Each test substance was tested in at least two cells for every concentration. All experiments were performed at room temperature.

Data analysis. Data acquisition and analyses were performed using the QPatch Assay software. The average of current amplitude values recorded from 4 sequential voltage pulses were used to calculate for each cell the effect of the test substance by calculating the residual current (% control) compared with vehicle pre–treatment and the % of inhibition (Eq. (8)).

The normalized data were plotted against the concentration of compound. The –Log of concentrations of compounds required to decrease current by 50% (pIC_{50}) were determined by fitting the data to a Hillequation with n ≥ 2

$$I/I_0 = 1/[1 + ([C]/IC50)^{nH}], \quad \text{with } pIC_{50} = -\log IC_{50} \quad (8)$$

where I_0 and I are the current amplitudes measured in the absence and presence of test compound, respectively, [C] is the concentration of compound in the external solution and nH is the Hill coefficient.

3.4. Study of photostability

Each UV-filter incorporated in an oil-in-water (O/W) emulsion were spread on PMMA plate and irradiated with a solar simulator applying different UVA-dose equivalent to an effective erythema radiant exposure of 120 kJ/m^2. The spectral transmittance of thin film of sunscreen was measured before and after sunlight exposure from 290 to 400 nm. The residual percentage of SPF in vitro (% $SPF_{eff.}$) and UVA-PF (% UVA-$PF_{eff.}$)) were calculated according to Eqs. (9) and (10) respectively. In fact, a filter is considered photostable if % $SPF_{eff.}$ and % UVA-$PF_{eff.}$ are more than or equal to 80.

$$\%SPF_{eff.} = in\ vitro SPF_{after}/in\ vitro SPF_{before} \times 100 \quad (9)$$

$$\%UVA - PF_{eff} = UVA - PF_{after}/UVA - PF_{before} \times 100 \quad (10)$$

4. Conclusions

The development of ltifunctional compounds is of great importance due to the correlation of biological networks. For this purpose, a series of benzothiazole derivatives was synthesized and investigated for its *in vitro* sunscreen UV-filter capacity, antioxidant, antifungal and antiproliferative activities. Regarding sunscreen UV-filter capacity, compounds **4g**, **4h**, **4k**, **11d**, **11g**, **11o** and **11r** could be considered as broad-spectrum and also UVA-filter compounds since their λc ≥ 370 nm and the UVA-PF value of each compound was greater than 1/3 of its SPF value. While compounds **4d** and **4j** were potential compounds for UVB protection. In addition, photostability studies showed that all synthesized compounds are photostable especially **11e** with a degradation rate less than 2%. In terms of antioxidant activity, compounds of classes **F** and **H**, characterized respectively by the presence of two hydroxyl groups in positions 3,4 and 2,5 of the 2-aryl ring showed good antioxidant profile. According to antifungal activity, compound **4h** showed the highest activity against all five dermatophytes, in particular against *Microsporum gypseum, Trichophyton tonsurans* and *Epidermophyton floccosum*. Moreover, significant activity was also observed for compounds **4f** and **4g** against *Microsporum gypseum* and *Epidermophyton floccosum.* With regard to the antiproliferative activity, compounds **4g** and **4k** are the potential compounds against CEM and SK-Mel 5 tumor cells, however, **4k** showed the best activity: it was respectively 6-fold more selective for CEM and 25-fold more selective toward SK-Mel 5 cells. Furthermore, compounds **4e**, **11n** and **11o** were respectively 15, 18 and 5 fold more selective toward Mia-Paca-2 cells. Considering that inhibition of HERG channels reduces proliferation and impairs invasiveness in several cancer cell types, hERG channels expressed in HEK cells can be target receptor for compounds with good anticancer activity. In these regards we may conclude that compound **4g** could be the potential candidate for blocking hERG potassium channels.

Taking into account all the biological evaluation, **4g** and **4k** could be potential compounds for the design of multifunctional drugs because

of their various biological activities. In addition, the benzothiazole derivatives could have a possible application as drugs for the treatment of neoplastic diseases including childhood leukemia, pancreatic cancer and melanoma. All together the data obtained have highlighted interesting activities sufficient to propose this scaffold as potential usefulness in the design of multifunctional compounds. Finally, the activity on **Mia-Paca-2, SK-Mel5** and **CEM** cells paralleled by hERG channel inhibition warrant further investigation because of the importance in antitumor therapy.

Declaration of Competing Interest

The authors declare that they have no known competing financial interests or personal relationships that could have appeared to influence the work reported in this paper.

Acknowledgment

This work was supported by University of Ferrara (Grant FAR 2017 to SM and SV) and the Ministry of Education University and Research of Italy (grant PRIN 2017E84AA4_002 to SM) and Ambrosialab srl (Ferrara, Italy); the scholarship to ES was kindly supported by APTUIT (Verona, Italy). We thank Selena Nola for doing the hERG study.

Appendix A. Supplementary material

Supplementary data to this article can be found online at https://doi.org/10.1016/j.bioorg.2020.103960.

References

[1] Y. Fang, H. Zhou, Q. Gu, J. Xu, Synthesis and evaluation of tetrahydroisoquinoline-benzimidazole hybrids as multifunctional agents for the treatment of Alzheimer's disease, Eur. J. Med. Chem. 167 (2019) 133–145.
[2] A. Baldisserotto, M. Demurtas, I. Lampronti, D. Moi, G. Balboni, S. Vertuani, S. Manfredini, V. Onnis, Benzofuran hydrazones as potential scaffold in the development of multifunctional drugs: Synthesis and evaluation of antioxidant, photoprotective and antiproliferative activity, Eur. J. Med. Chem. 156 (2018) 118–125.
[3] F. Afaq, V.M. Adhami, H. Mukhtar, Photochemoprevention of ultraviolet B signaling and photocarcinogenesis, Mutat. Res. 571 (2005) 153–173.
[4] G.T. Wondrak, M.K. Jacobson, E.L. Jacobson, Endogenous UVA photosensitizers: mediators of skin photodamage and novel targets for skin photoprotection, Photochem. Photobiol. Sci. 5 (2006) 215–237.
[5] N. Saewan, A. Jimtaisong, Photoprotection of natural flavonoids, J. Appl. Pharama. Sci. 3 (2013) 129–141.
[6] S. Courdavault, C. Baudouin, M. Charveron, B. Canguilhem, A. Favier, J. Cadet, T. Doukia, Repair of the three main types of bipyrimidine DNA photoproducts in human keratinocytes exposed to UVB and UVA radiations, DNA Repair. 4 (2005) 836–844.
[7] D. Mitchell, A. Fernandez, The photobiology of melanocytes modulates the impact of UVA on sunlight-induced melanoma, Photochem. Photobiol. Sci. 11 (2012) 69–73.
[8] M.E. Inal, A. Kahramant, T. Kkent, Beneficial effects of quercetin on oxidative stress induced by ultraviolet A, Clin. Exp. Dermatol. 26 (2001) 536–539.
[9] M. Wlaschek, I. Tantcheva-Poor, L. Naderi, W. Ma, L.A. Schneider, Z. Razi-Wolf, J. Schuller, K. Scharffetter-Kochanek, Solar UV irradiation and dermal photoaging, J. Photochem. Photobiol. B. 63 (2001) 41–51.
[10] Hossam El-Din M. Omar. Mycotoxins-Induced Oxidative Stress and Disease, Chapter 3, http://dx.doi.org/10.5772/51806.
[11] L.A. Corcuera, S. Amézqueta, L. Arbillaga, A. Vettorazzi, S. Touriño, J.L. Torres, A. Lopéz de Cerain, A polyphenol-enriched cocoa extract reduces free radicals produced by mycotoxins, Food Chem. Toxicol. 50 (2012) 989–995.
[12] A. Bino, A. Baldisserotto, E. Scalambra, V. Dissette, D.E. Vedaldi, A. Salvador, E. Durini, S. Manfredini, S. Vertuani, Design, synthesis and biological evaluation of novel hydroxy-phenyl-1H-benzimidazoles as radical scavengers and UV-protective agents, J. Enzyme Inhib. Med. Chem. 32 (2017) 527–537.
[13] S. Kumar, D.S. Rathore, G. Garg, K. Khatri, R. Saxena, S.K. Sahu, Synthesis and evaluation of some benzothiazole derivatives as antidiabetic agents, Int. J. Pharm. Pharm. Sci. 9 (2017) 60–68.
[14] R.S. Keri, C. Quintanova, S.M. Marques, A.R. Esteves, S.M. Cardoso, M.A. Santos, Design, synthesis and neuroprotective evaluation of novel tacrine–benzothiazole hybrids as multi-targeted compounds against Alzheimer's disease, Bioorg. Med. Chem. 21 (2013) 4559–4569.
[15] N. Gupta, N. Ajmera, R. Gautam, D. Sharma, Gauatam, Novel synthesis and biological activity study of pyrimido [2,1-b] benzothiazoles, Ind. J. Chem. 48B (2009) 853–858.
[16] R.M. Kumbhare, V.N. Ingle, Synthesis of novel benzothiozole and benzisoxazole functionalized unsymmetrical alkanes and study of their antimicrobial activity, Ind. J. Chem. 48B (2009) 996–1000.
[17] Y. Murthi, D. Pathak, Synthesis and Antimicrobial screening of Substituted 2-Mercaptobenzothiazoles, J. Pharm. Res. 7 (2008) 153–155.
[18] M. Maharan, S. William, F. Ramzy, A. Sembel, Synthesis and in vitro Evaluation of new benzothiazolederivaties as schistosomicidal agents, Molecules 12 (2007) 622–633.
[19] B. Rajeeva, N. Srinivasulu, S. Shantakumar, Synthesis and Antimicrobial activity of some new 2-substituted benzothiazole derivatives, E-J. Chem. 6 (2009) 775–779.
[20] S. Agarwal, D.K. Agarwal, N. Gautam, K. Agarwal, D.C. Gautam, Synthesis and in vitro antimicrobial evaluation of benzothiazole incorporated thiazolidin-4-ones derivatives, J. Korean Chem. Soc. 58 (2014) 33–38.
[21] M.K. Singh, R. Tilak, G. Nath, S.K. Awasthi, A. Agarwal, Design, synthesis and antimicrobial activity of novel benzothiazole analogs, Eur. J. Med. Chem. 63 (2013) 635–644.
[22] S.K. Rangappa, M.R. Patil, S.A. Patil, S. Budagumpi, A comprehensive review in curren developments of benzothiazolebased molecules in medicinal chemistry, E. J. Med. Chem. 89 (2015) 207e251.
[23] J.C. Chen, L. Qian, Y. Shen, L.M. Chen, K.C. Zheng, A QSAR study and molecular design of benzothiazole derivatives as potent anticancer agents, Sci. China Ser. B-Chem. 51 (2008) 111–119.
[24] A.L. Loaiza-Pérez, V. Trapani, C. Hose, S.S. Singh, J. Trepel, M.F.G. Stevens, T.D. Bradshaw, E.A. Sausville, The aryl hydrocarbon receptor mediates sensitivity of MCF-7 breast cancer cells to the antitumor agent 2-(4-amino-3-methylphenyl)benzothiazole, Mol. Pharmacol. 61 (2002) 13–19.
[25] V. Trapani, V. Patel, H.P. Ciolino, G.C. Yeh, C. Hose, J.B. Trepel, M.F.G. Stevens, E.A. Sausville, A.L. Loaiza-Pérez, DNA damage and cell cycle arrest induced by 2-(4-amino-3-methylphenyl)-5-fluorobenzothiazole (5F 203, NSC 703786) is attenuated in aryl hydrocarbon receptor deficient MCF-7 cells, Br. J. Cancer 88 (2003) 599–605.
[26] R. Caputo, M.L. Calabro, N. Micale, A.D. Schimmer, M. Ali, M. Zappala, S. Grasso, Synthesis of benzothiazole derivatives and their biological evaluation as anticancer agents, Med. Chem. Res. 21 (2012) 2644–2651.
[27] M. Yoshida, I. Hayakawa, N. Hayashi, T. Agatsuma, Y. Oda, F. Tanzawa, S. Iwasaki, K. Koyama, H. Furukawa, S. Kurakatad, Y. Sugano, Synthesis and biological evaluation of benzothiazole derivatives as potent antitumor agents, Bioorg. Med. Chem. Lett. 15 (2005) 3328–3332.
[28] E.L. Stone, F. Citossi, R. Singh, B. Kaur, M. Gaskell, P.B. Farmer, A. Monks, C. Hose, M.F. Stevens, C.O. Leong, M. Stocks, B. Kellam, M. Marlow, T.D. Bradshaw, Antitumour benzothiazoles. Part 32: DNA adducts and double strand breaks correlate with activity; synthesis of 5F203 hydrogels for local delivery, Bioorg. Med. Chem. 23 (2015) 6891–6899.
[29] J. Ma, G. Bao, L. Wang, W. Li, B. Xu, B. Du, J. Lv, X. Zhai, P. Gong, Design, synthesis, biological evaluation and preliminary mechanism study of novel benzothiazole derivatives bearing indole-based moiety as potent antitumor agents, Eur. J. Med. Chem. 96 (2015) 173–186.
[30] M.F.G. Stevens, C.J. McCall, P. Lelieveld, P. Alexander, A. Richter, D.E. Davies, Structural studies on bioactive compounds. 23. Synthesis of polyhydroxylated 2-phenylbenzothiazoles and a comparison of their cytotoxicities and pharmacological properties with genistein and quercetin, J. Med. Chem. 37 (1994) 1689–1695.
[31] A.A. Mohammed, D. Loganathan, C.M. Charu, S. Sumit, Synthesis and biological evaluation of some novel pyrazolopyrimidines incorporating a benzothiazole ring system, Acta Pharm. 63 (2013) 19–30.
[32] K. Vishal, S. Saurabh, H. Asif, Synthesis and in vivo Anti-inflammatory and Analgesic activities of Oxadiazoles clubbed with Benzothiazole nucleus, Int. Curr. Pharmaceut. J. 4 (2015) 457–461.
[33] N. Siddiqui, A. Rana, S.A. Khan, M.A. Bhat, S.E. Haque, Synthesis of benzothiazole semicarbazones as novel anticonvulsants—The role of hydrophobic domain, Bioorg. Med. Chem. Lett. 17 (2007) 4178–4182.
[34] D.C. Liu, X.Q. Deng, S.B. Wang, Z.S. Quan, Synthesis and anticonvulsant activity evaluation of 7-alkoxy[1,2,4]triazolo[3,4-b]benzothiazol-3(2H)-ones, Arch. Pharm. Chem. Life Sci. 347 (2014) 268–275.
[35] M.Z. Hassan, S.A. Khan, M. Amir, Design, synthesis and evaluation of N-(substituted benzothiazol-2-yl)amides as anticonvulsant and neuroprotective, Eur. J. Med. Chem. 58 (2012) 206–213.
[36] V.G. Ugale, H.M. Patel, S.G. Wadodkar, S.B. Bari, A.A. Shirkhedkar, S.J. Surana, Quinazolino-benzothiazoles: Fused pharmacophores as anticonvulsant agents, Eur. J. Med. Chem. 53 (2012) 107–113.
[37] R.I. Cuevas-Hernández, J. Correa-Basurto, C.A. Flores-Sandoval I.I. Padilla-Martínez, B. Nogueda-Torres, M. de L. Villa-Tanaca, F. Tamay-Cach, J.J. Nolasco-Fidencio, J.G. Trujillo-Ferrara, Fluorine-containing benzothiazole as a novel trypanocidal agent: design, in silico study, synthesis and activity evaluation, Med. Chem. Res. 25 (2016) 211–224.
[38] B. Chi, C. Jill, P. David, J. Song, W. Choy, P. Lambert, D. Gagne, Discovery of benzothiazole derivatives as efficatious and enterocyte-specific MTP inhibitors, Bioorg. Med. Chem. Lett. 19 (2009) 1416–1420.
[39] C.A. Mathis, Y. Wang, D.P. Holt, G.-F. Huang, M.L. Debnath, W.E. Klunk, Synthesis and evaluation of 11C-labeled 6-substituted 2-arylbenzothiazoles as amyloid imaging agents, J. Med. Chem. 46 (2003) 2740–2754.
[40] P.S. Yadav, D. Devprakash, G.P. Senthilkumar, Benzothiazole: different methods of synthesis and diverse biological activities, Int. J. Pharm. Sci. Drug. Res. 3 (2011) 1–7.
[41] M.R. Chedekel, P. PohAgin, R.M. Sayre, Photochemistry of pheomelanin: action spectrum for superoxide production, Photochem. Photobiol. 31 (1980) 553–555.
[42] K. Herrmann, Occurrence and content of hydroxycinnamic and hydroxybenzoic

acid compounds in foods, Crit. Rev. Food Sci. Nutr. 28 (1989) 315–347.
[43] Z.A. Velkov, M.K. Kolev, A.V. Tadjer, Modeling and statistical analysis of DPPH scavenging activity of phenolics, Collect. Czech. Chem. Commun. 72 (2007) 1461–1471.
[44] A.A. Weekes, M. Bagley, A.D. Westwell, An efficient synthetic route to biologically relevant 2-phenylbenzothiazoles substituted on the benzothiazole ring, Tetrahedron 67 (2011) 7743–7747.
[45] M. Hiroharu, O. Nobuhiro, M. Masahiko, S. Hiroshi, M. Katsuhito, M. Noriaki, T. Keiichiro, K. Nobuaki, A. Toshio, T. Yasuhisa, Y. Keiichi, K. Toshio, Antirheumatic agents: novel methotrexate derivatives bearing a benzoxazine or benzothiazine moiety, J. Med. Chem. 40 (1997) 105–111.
[46] J. Dey, S.K. Dogra, Electronic absorption and fluorescence spectra of 2-phenyl-substituted benzothiazoles: study of excited-state proton transfer reactions, Can. J. Chem. 69 (1991) 1539–1547.
[47] B.L. Diffey, J. Robson, A new substrate to measure sunscreen protection factors throughout the ultraviolet spectrum, J. Soc. Cosmet. Chem. 40 (1989) 127–133.
[48] J.D. Fourneron, F. Faraud, A. Fauneron, Sur la mesure in vitro de la protection solaire de crèmes cosmétiques, C. R. Acad. Sci. II, Paris 2 (1999) 421–427.
[49] M. Pissavini, L. Ferrero, V. Alaro, U. Heinrich, H. Tronnier, D. Kockott, D. Lutz, V. Tournier, M. Zambonin, M. Meloni, Determination of the in vitro SPF, Cosmet. Toiletries, Oak Park. 118 (2003) 63–72.
[50] A. Dimitrovska Cvetkovska, S. Manfredini, P. Ziosi, S. Molesini, V. Dissette, I. Magri, C. Scapoli, A. Carrieri, E. Durini, S. Vertuani, Factors affecting SPF in vitro measurement and correlation with in vivo results, Int. J. Cosmet. Sci. 39 (2017) 310–319.
[51] SPF Calculator Software (version 2.1), Shimadzu, Milan (Italy).
[52] US Food and Drug Administration, 21 CFR Parts 347 and 352, Sunscreen Drug Products for Over-the-Counter Human Use; Proposed Amendment of Final Monograph, Silver Spring, MD (USA), 2007, https://www.fda.gov/ OHRMS/DOCKETS/98fr/cd031.pdf (accessed April 25, 2017).
[53] D. Garoli, M.G. Pelizzo, B. Bernardini, P. Nicolosi, M. Alaibac, Sunscreen tests: Correspondence between in vitro data and values reported by the manufacturers, J. Dermatol. Sci. 52 (2008) 193–204.
[54] A.M. Farrelly, S. Ro, B.P. Callaghan, M.A. Khoyi, N. Fleming, B. Horowitz, K.M. Sanders, K.D. Keef, Expression and function of KCNH2 (HERG) in the human jejunum, Am. J. Physiol. Gastrointest. Liver Physiol. 284 (2003) 883–895.
[55] J.E. Brayden, M.T. Nelson, Regulation of arterial tone by activation of calcium-dependent potassium channels, Science 256 (1992) 532–535.
[56] M.E. Laniado, S.P. Fraser, M.B. Djamgoz, Voltagegated K (+) channel activity in human prostate cancer cell lines of markedly different metastatic potential: Distinguishing characteristics of PC-3 and LNCaP cells, Prostate 46 (2001) 262–274.
[57] K. Preussat, C. Beetz, M. Schrey, R. Kraft, S. Wolfl, R. Kalff, S. Patt, Expression of voltage-gated potassium channels Kv1.3 and Kv1.5 in human gliomas, Neurosci. Lett. 346 (2003) 33–36.
[58] X.T. Wang, Y. Nagaba, H.S. Cross, F. Wrba, L. Zhang, S.E. Guggino, The mRNA of L-type calcium channel elevated in colon cancer: Protein distribution in normal and cancerous colon, Am. J. Pathol. 157 (2000) 1549–1562.
[59] A. Cherubini, G.L. Taddei, O. Crociani, M. Paglierani, A.M. Buccoliero, L. Fontana, I. Noci, P. Borri, E. Borrani, M. Giachi, A. Becchetti, B. Rosati, E. Wanke, M. Olivotto, A. Arcangeli, HERG potassium channels are more frequently expressed in human endometrial cancer as compared to non-cancerous endometrium, Br. J. Cancer 83 (2000) 1722–1729.
[60] A.P. Hegle, D.D. Marble, G.F. Wilson, A voltage-driven switch for ion independent signaling by ether-à-go-go K+ channels, Proc. Natl. Acad. Sci. USA 103 (2006) 2886–2891.
[61] E. Afrasiabi, M. Hietamäki, T. Viitanen, P. Sukumaran, N. Bergelin, K. Törnquist, Expression and significance of HERG (KCNH2) potassium channels in the regulation of MDA-MB-435 S melanoma cell proliferation and migration, Cell Signal. 22 (2010) 57–64.
[62] J.J. Babcock, M. Li, hERG channel function: beyond long QT, Acta Pharmacol. Sin. 34 (2013) 329–335.
[63] M. Wang, J. Li, M. Rangarajan, Y. Shao, E.J. La Voie, T.-C. Huang, C.-T. Ho, Antioxidative phenolic compound from sage (salvia officinalis), J. Agric. Food Chem. 46 (1998) 4868–4873.
[64] I.F.F. Benzie, J.J. Strain, The ferric reducing ability of plasma as a measure of antioxidant power: the FRAP assay, Anal. Biochem. 239 (1996) 70–76.
[65] S.G. Rezende, J.G. Dourado, F.M.A. Lino, D.C. Vinhal, E.C. Silva, E.S. Gil, Methods used in evaluation of the sun protection factor of sunscreens. REF-ISSN1808-0804, revista electronic de farmàcia XI (2014) 37–54.
[66] C. Romagnoli, A. Baldisserotto, C.B. Vicentini, D. Mares, E. Andreotti, S. Vertuani, S. Manfredini, Antidermatophytic action of resorcinol derivatives: ultrastructural evidence of the activity of phenylethyl resorcinol against *Microsporum gypseum*, Molecules. 21 (2016) 1306.